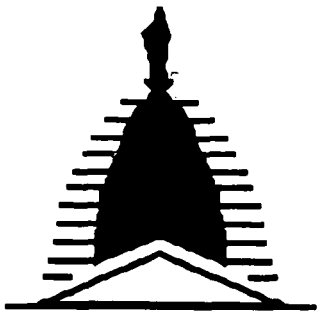

UNIVERSITY of
NOTRE DAME

NASA/USRA UNIVERSITY ADVANCED DESIGN PROGRAM 1990-1991

UNIVERSITY SPONSOR
BOEING COMMERCIAL AIRPLANE COMPANY

FINAL DESIGN PROPOSAL

BETA SYSTEMS - EL TORO

A Proposal in Response to a Commercial Air Transportation Study

May 1991

Department of Aerospace and Mechanical Engineering
University of Notre Dame
Notre Dame, IN 46556

" EL TORO "

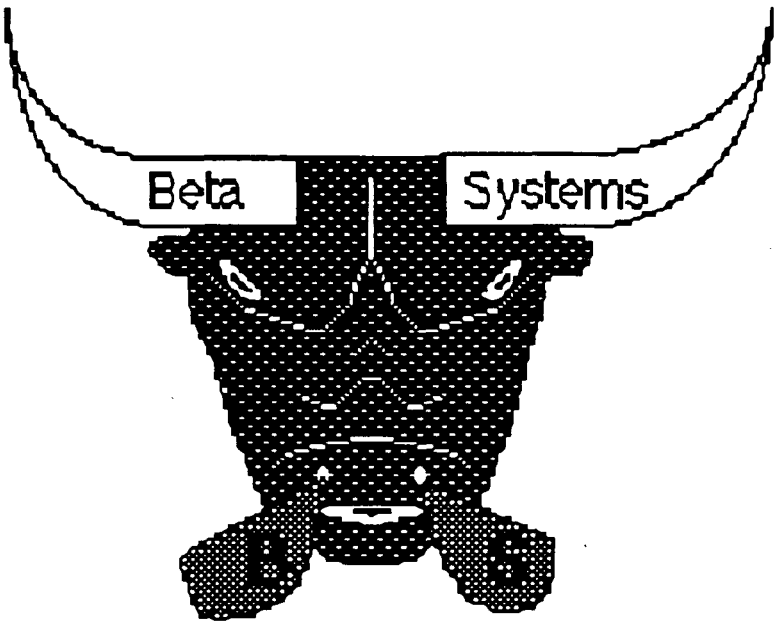

Beta Systems

Steve Muenzberg	**Project Manager/ Performance Lead**
Shane Gillespie	**Aerodynamics Lead**
Jim Coogan	**Propulsion Lead**
Pat Monahan	**Weights Lead**
Liam Bruen	**Stability & Control Lead**
Bob Wincer	**Structures Lead**
Rob Wilkey	**Economics Lead**

EXECUTIVE SUMMARY

El Toro is a remotely piloted airplane that has been designed to operate as a commercial transport in a fictional "Aeroworld" where the passengers are ping pong balls and distances between cities are on the order of thousands of feet. A successful design for this mission is an airplane that can profitably meet the needs of the "Aeroworld" market for both the manufacturer and the airlines.

From mission studies that were conducted on the "Aeroworld" market, it was determined that an aircraft range of 6000 feet plus loiter time would be able to serve about 90% of the market. It was also determined from these studies that an aircraft capacity of about 50 passengers would best meet the needs of the market. El Toro meets both of these market requirements with a range of 25000 feet and a capacity of 51 passengers. The cruise altitude will be 20 feet and El Toro will be able to perform a sustained, level 60 feet radius turn.

The present design for El Toro will profitably meet the requirements for operation in "Aeroworld" with a ticket price comparable to the ticket prices of current transportation. The extended range of El Toro allows for numerous flights to be flown before the battery pack needs to be changed. This drastically reduces the operating costs to the airlines allowing them to charge less for a ticket or else to realize a higher profit margin. The unit production cost for the airplane is estimated to be $162,000, including all material, systems and labor.

The airfoil selected for El Toro is the Spica chosen for its high lift coefficient at low Reynold's number and its ease of construction. The wing of El Toro is sized for minimum power required during cruise while meeting structural limitations. The wing has a span of 8.33 feet, an area of 1000 square inches, and an aspect ratio of 10. There is no sweep or twist associated with the wing and the taper ratio is 1.0. The wing is hinged at 2 feet on either side of the fuselage to allow El Toro to fold the wing while on the ground and enter any airport gate.

The propulsion system for El Toro was sized for take-off to allow the airplane to take off in 60 feet with enough extra power to overcome changes in runway conditions, aircraft weight and aircraft aerodynamics. The propulsion system for El Toro consists of a propeller-electric motor combination with the prop mounted at the front of the fuselage. The propeller, the Zinger 10-6, is driven by an Astro-15 Cobalt motor and twelve P-120SCRP battery cells having a total capacity of 1200 MAH. The system is capable of 100 watts of power and has throttling capabilities.

Maximum passenger comfort and safety established a majority of the stability and control design requirements. A data base of other

civil aircraft led to the choice of a conventional aft horizontal and vertical tail. This arrangement provides not only proven results but adds to passenger comfort through a smooth ride. Longitudinal stability and control will be achieved with the horizontal tail with elevator. Directional stability and control will be achieved with an aft vertical tail with a rudder. Lateral stability will be achieved with a high wing with dihedral. Ailerons are not used because of the hinged wings.

Some areas of concern are in the construction of the folding wing, placement of the center of gravity, and the fact that Beta Systems is inexperienced at airplane construction.

One of the most critical areas in this airplane's structural configuration is the hinge design of the wing. The feasibility of this technology must be demonstrated in order to justify the airplane design, for without folding wings, El Toro would not meet the gate requirements of Aeroworld. One of the primary purposes of the technology demonstrator will be to show that a working folding wing can be constructed.

Placement of the center of gravity is always a critical concern when transferring a design from paper to actual construction. In order to insure that the actual center of gravity is located at the desired location, the fuel will be moveable inside the fuselage. This will allow for adequate center of gravity control.

The inexperience of Beta Systems in airplane construction has been taken into account throughout the whole design process. Design decisions were constantly made with this concern in mind, resulting in an airplane that is relatively straight forward to construct and that will be reliable in the field.

Beta Systems is confident that El Toro will be a successful and profitable airplane in Aeroworld for both the manufacturer and the airlines. This success will continue into the future with a family of derivative aircraft. Possible derivatives will have extended or shortened fuselages, larger or smaller engines, or capabilities to be converted for cargo or military applications. The success of El Toro is limitless.

A three-view drawing and a specifications summary follow this executive summary.

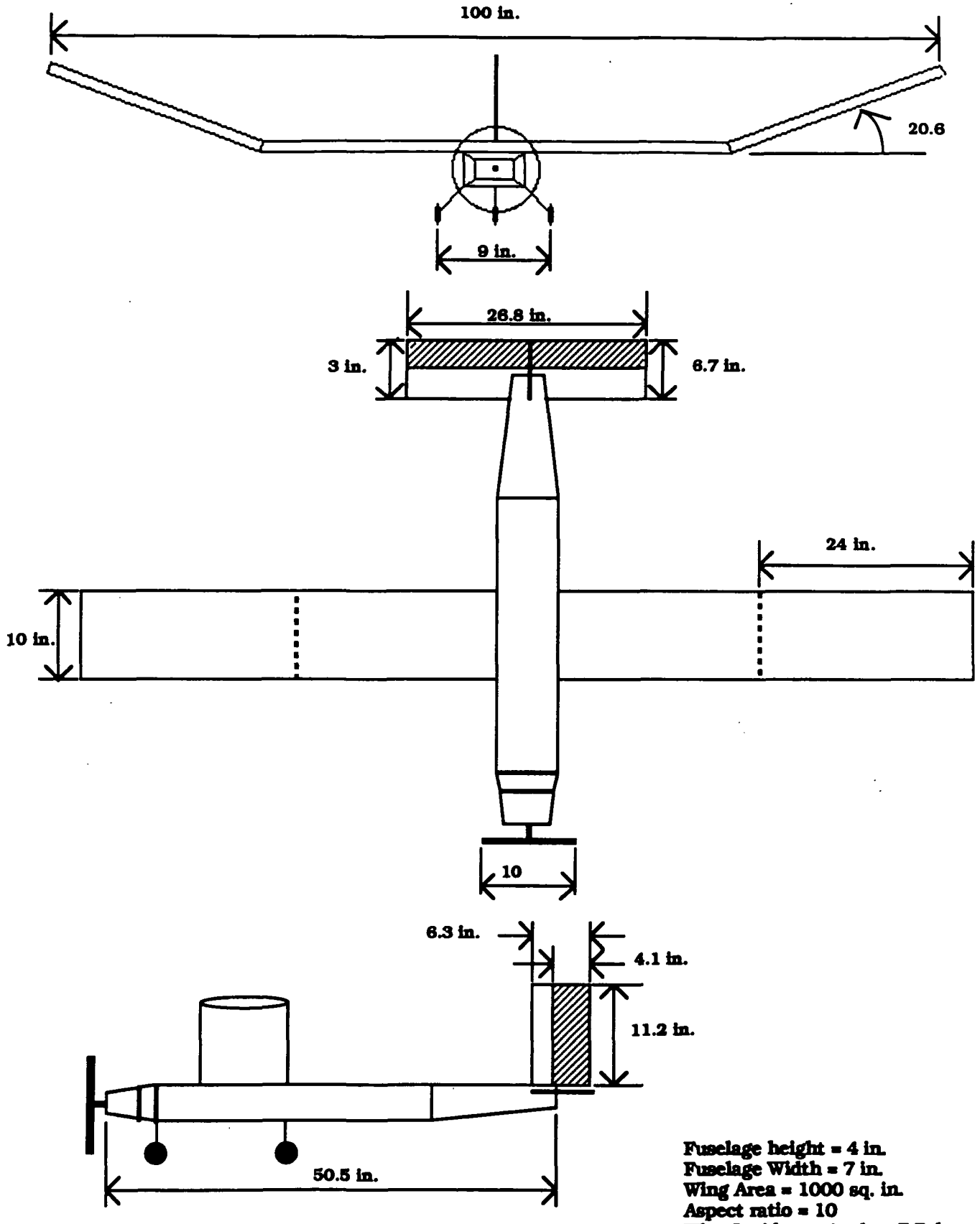

Fuselage height = 4 in.
Fuselage Width = 7 in.
Wing Area = 1000 sq. in.
Aspect ratio = 10
Wing Incidence Angle = 7.7 deg.
Weight = 80 oz.
Control : Rudder and Elevator
Engine : Astro Cobalt 15 - Geared
Propeller : Zinger 10-6

SCALE : 1 in. = 15 in.

SPECIFICATIONS SUMMARY

Performance		
	Endurance (at cruise)	16.3 min.
	Endurance (max)	16.6 min.
	Range (at cruise)	25,000 feet
	Range (max)	33,000 feet
	Stall Velocity	22.8 ft/s
	Max Velocity	76.5 ft/s
	Max Rate of Climb	870 ft/min
	Max Power Available	100 W
	Max Roll Rate	30.0 deg/s
	Min Glide Angle	-3.5 deg
	Min Take-off Distance	23.8 ft
Configuration		
	Wing Span	100. in
	RPV legnth	50.5 in.
	Weight	80.0 oz.
Wing		
	Airfoil	Spica
	Angle of Incidence	7.7 deg
	Aspect Ratio	10
	Chord	10. in.
	Equivelant Dihedral	13. deg
	Taper Ratio	1
Fuselage		
	Cross-section	7in. x 4. in.
	Payload Volume	700. $in.^3$
Empennage		
	Airfoil sections	Flat Plate
	Horizontal Tail Area	180. $in.^2$
	H. Tail Aspect Ratio	4
	Tail angle of incidence	1.3 deg
	Elevator Area	81. $in.^2$
	Vertical Tail Area	71. $in.^2$
	V. Tail Aspect Ratio	2.75

	Rudder Area	46.2 $in.^2$
Motor		
	Motor Type	Astro 15
	Battery Pack	P-120 SCRP
	Static Thrust	6.16 N
	Propeller	Zinger 10-6
	Propeller Efficiency	.71 (cruise)
Economics		
	Operating Cost / passenger	$3.80-$5.69/50 ft
	Ticket Price (+ $50 flat rate)	$7.32-$11.10/50ft
	Construction Cost (prototype)	$203,700

TABLE OF CONTENTS

A. MISSION STUDY

A.1 INTRODUCTION

The goal of the airplane design process is to maximize the overall effectiveness and profit of a commercial transport in the new airplane market of Aeroworld. In this new market, the current competition for travel is provided by train and ship transportation. A market thus exists for a faster and more comfortable form of transportation, the airplane.

From the market data that is provided for Aeroworld, it is determined that approximately 90% of the travel occurs within distances of 6000 feet or less. In addition, the farthest two cities are less than 10000 feet apart, within twice the 6000 feet distance. Most of the market can be served with a direct flight while the rest of the market can be served with only one intermittent stop. For these two reasons a flight range of 6000 feet is chosen.

In order to meet the needs of Aeroworld the airplane must be affordable to the average traveler. In determining the ticket price for a flight, it is assumed that the inhabitants of Aeroworld are willing to pay a higher fare for the benefit of trip time savings that the airplane will provide. Thus, a ticket price of approximately twice the cost of the train is set as the price goal. The cost per flight for the operation of the aircraft was calculated using the most conservative guidelines assuming the highest fuel costs and a battery change for every flight. This per flight operating cost was divided by the target ticket price to determine the minimum number of people needed on a flight to cover

the operating costs. It was determined that a capacity of 30 people per flight would cover the operating costs and provide a reasonable profit for the airlines. This minimum number will decrease if the cost of fuel is less or if a battery change is not needed, in which case the ticket price could be lowered or the profit margin increased. The market exists, however, for a capacity of up to 60 people per flight. Thus, the capacity of the airplane will be between 30 and 60 people.

The strictest limitation on the capacity of the airplane does not have to do with the available market but with the size limitation of the airplane. The airplane must be able to fit into a five foot gate in order to be able to make use of all of the available gates and thus serve the most people. This gate size limitation places a limit on the size of the entire airplane, which thus limits the number of passengers that can fit comfortably into the fuselage. This size limitation will ultimately determine the exact number between 30 and 60 people that the airplane will be capable of carrying.

As a passenger airplane, the design must allow for maximum passenger comfort in flight as well as on the ground. In order to provide in-flight comfort and reliability, a conventional control scheme will be chosen. The philosophy behind this is that conventional controls are a proven technology and prove to provide a smooth ride for the passengers. Operating with a single forward mounted engine is another proven technology that will minimize risks associated with new technology.

In order to provide comfort on the ground, a rapid turn around time for the aircraft is essential. Thus, the battery pack and systems

operations must be easily accessible. A tricycle landing gear will provide the smoothest ride during take off and landing.

Two final requirements for the proposed airplane are flight speed and takeoff distance. The flight speed of the airplane will be Mach 0.8 in order to make each trip as fast as possible while still complying with the noise requirements of Aeroworld. The takeoff distance for the airplane will be less than 60 feet in order to serve the majority of the market. An airplane with this takeoff distance will be able to serve all of the cities except C and O. Future derivative aircraft could possibly have the capability of serving these two cities as well.

The above mission analysis provides the guidelines and justifications for the following Design Requirements and Objectives:

A.2 DESIGN REQUIREMENTS AND OBJECTIVES

1. Range = 6000 feet plus diversion to nearest airport and loiter
2. Affordable ticket prices
2. Capacity = 30-60 passengers
3. Fit into 5 ft. gates
4. Takeoff in 60 feet or less
5. Tricycle landing gear
6. Easy Battery Access
7. Single electric engine (forward mounted)
8. Conventional control surfaces

B. ECONOMICS

At the outset of this project pertinent information regarding Aeroworld was provided in the Request for Proposal. The goal, from an economic view, is to utilize this information to maximize the return on investment gained by any airline purchasing the aircraft. The information necessary for the economic analysis is the number of passengers traveling between cities, the distance between cities, and ticket prices for existing train and ship transportation. The total number of passengers traveling in Aeroworld is broken into four distance categories and the percentage of passengers in these categories is shown in Figure B.1 below.

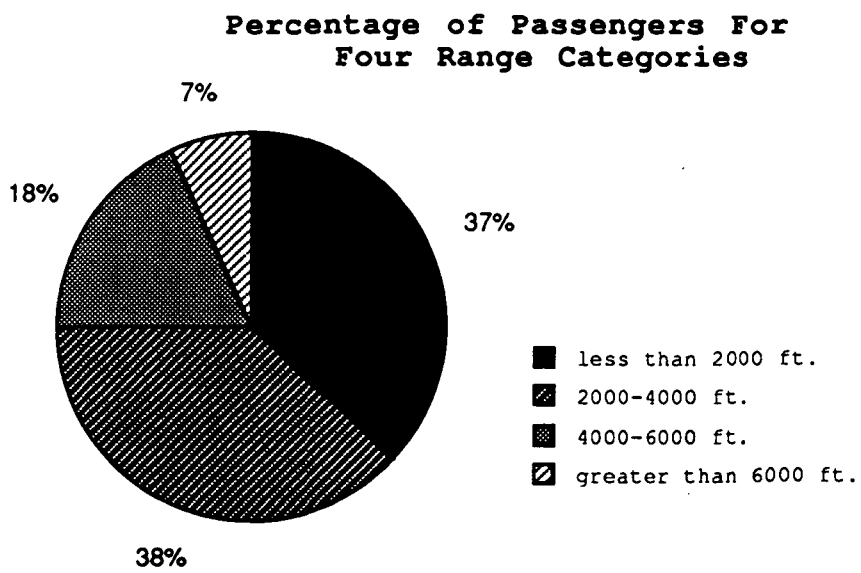

Figure B.1

From this graph it can be seen that ninety-three percent of the passengers want to fly to destinations less than six thousand feet. The farthest two cities in Aeroworld are ten thousand feet apart, which means that a range of six thousand feet would allow the aircraft to fly anywhere in Aeroworld with only one intermediate stop. From this information it was determined that a market of short to medium range exists for maximum profit.

Since other modes of transportation already exist in Aeroworld it is assumed that the primary desire for air travel stems from the fact that people want to travel more quickly. It was also decided that each aircraft would be able to complete four round trip flights per day in an assumed sixteen-hour flying day. It was determined that a Mach Number of 0.8 was the desired flight speed. With this flight speed it will be possible to achieve a good balance between speed and cost.

In determining the number of passengers it was found that the market exists for thirty to sixty passengers per flight. It is estimated that it would cost $ 250,000 to build such an aircraft. The primary economic considerations in addition to production cost are the fuel and maintenance costs. Initially it was found that fuel cost for operation would be approximately $ 500 per fifty feet, and maintenance would be $ 1000 per battery change. It was believed that setting the ticket price for air travel at $ 12.50 per fifty feet plus $ 50 flat rate, twice that for the train, would be competitive due to the speed with which the aircraft could travel. In this conservative cost analysis it is determined that approximately thirty passengers are needed to break even on the cost of the operation of the aircraft.

As the design process advanced and more detailed information was obtained for size and performance it became necessary to perform a more in-depth economic analysis. Once again the primary considerations in the cost analysis were production cost, fuel cost, and maintenance cost. The first step in the economic analysis was to estimate the cost of producing the aircraft. In the request for proposal it is specified that one actual dollar spent on the technology demonstrator is equivalent to four hundred dollars in Aeroworld. Also, each man-hour taken for construction of the technology demonstrator would cost one hundred Aeroworld dollars. The unit production cost was determined to be $162,000, broken down as follows:

propulsion and controls	$ 60,000
speed controller	$ 40,000
materials	$ 50,000
labor (120 man-hours)	$ 12,000
TOTAL	$ 162,000

It was decided that Beta Systems would sell each aircraft for $231,000. This gives Beta Systems a profit of thirty percent enabling it to operate and is also a fair price for prospective investors. It is assumed that each aircraft will have a useful life of twenty years and investors will pay for the aircraft in ten years. Using an interest rate of twelve percent at ten years, the cost to the investor would be $3303.30 per month. It is estimated that each aircraft will make approximately 240 flights per month (4 round trip flights per day). This breaks down to approximately one dollar per passenger ticket.

To determine the ticket price for passengers it is necessary to determine the operating and maintenance cost for the aircraft. Given that the fuel price will range form $60 per milliamp-hour (mah) to $120 per milliamp-hour, it was determined that three price ranges would be established. Given that maintenance will cost $500 per minute and estimating that it will require two minutes for each battery change, a maintenance cost of $1000 per battery change was calculated. Dividing this $1000 by the total range (25,000 feet) of which the aircraft is capable, it was found that the cost for maintenance would be $2.00 per fifty feet.

Once the batteries were selected it became possible to calculate the fuel cost of the aircraft. The capacity of the battery cell arrangement selected was 1200 mah. Dividing this figure by the range of 25,000 feet determined that the battery usage would be 2.4 milliamp-hours per fifty feet. Multiplying this by the fuel price produces the fuel cost for operating the aircraft. In determining the ticket prices for the proposed aircraft it was decided that it would be desirable to break even on cost at fifty percent of the aircraft's capacity of fifty-one passengers. Therefore, the total cost (fuel + maintenance) for the longest flight (city A to city N - 9035.5 feet) was divided by twenty-five passengers. This ticket rate was then broken down to a cost per fifty feet and applied to all flights. The cost per flight is a function of fuel prices as seen in Figure B.2.

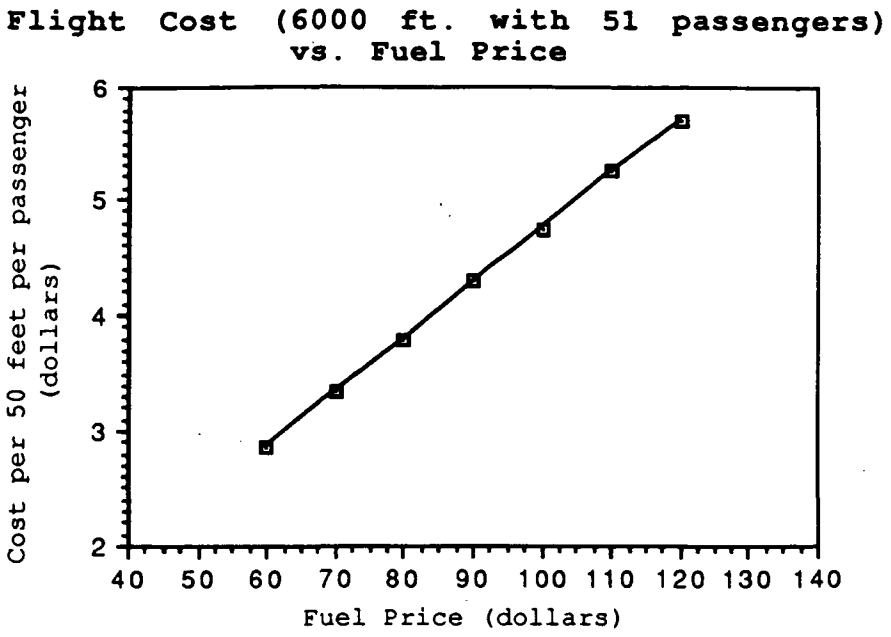

Figure B.2

From this information it was determined that the fuel prices would be divided into three categories (Fig. 2): (1) \$60-\$80 per mah; (2) \$81-\$100 per mah; and (3) \$101-\$120 per mah. The resulting fuel costs and ticket prices are as follows:

	Fuel Price 1 ($80/mah)	Fuel Price 2 ($100/mah)	Fuel Price3 ($120/mah)
Fuel Cost per 50 feet (6000 ft flight)	\$ 192.00	\$ 240.00	\$ 288.00
Maintenance cost per 50 feet (6000 ft flight)	\$ 2.00	\$ 2.00	\$ 2.00
Cost per 50 ft per passenger (full aircraft)	\$ 3.80	\$ 4.75	\$ 5.69
Air fare per 50 feet *	\$ 7.32	\$ 9.22	\$ 11.10

* all flights have an additional \$50 flat rate

Tables have been included in Appendix B for city-to-city air fare, flight cost, profit, number of passengers to break even, and passenger load factor for individual aircraft. The profit is calculated for an aircraft filled to capacity (51 passengers). Included in the appendix is an explanation of these tables and the method of calculation.

C. CONCEPT SELECTION

Initially, seven design concepts were proposed by Beta Group, one from each member of the design team. From these designs the benefits and weaknesses of each concept were examined. This preliminary process lead to the selection of three proposals which best fit our mission requirements. They are presented as figures C.1-C.3.

The first concept uses a conventional wing- aft tail design (as do the others). It has a high wing for stability, that can be removed for easy access to the battery pack and controller units. The wing span is 5 ft. long in order to fit within the 5 ft. gate requirement. It uses no ailerons, instead having outward portions of the wings with dihedral for turn and roll stability. It has a rectangular fuselage and a tricycle landing gear.

The second concept, like the first, uses a tricycle landing gear and rectangular fuselage. However, this design utilizes a low wing design with dihedral. No ailerons are used. The span of this wing is 100" long and is hinged so that the wings can fold up to fit into the 5 ft. gate.

The third design is again a high wing design, no ailerons, with dihedral starting at the root. This plane also uses a hinged wing design. It however differs from the previous two proposals in that it uses a tail dragger type landing gear and the fuselage is round instead of rectangular.

Although these three planes were quite similar in many respects, there were critical differences that needed to be further investigated

to determine which components would be combined to yield a group proposal that would utilize the benefits of each of the individual concepts. Certain characteristics were easily decided upon, such as a tricycle landing gear to provide the most comfort for our passengers. However, it was necessary to form three research teams to further examine three critical design areas .

These areas were:

High Wing vs. Low Wing

5 ft. Span vs Folding Wing

Circular vs Square (rectangular) Fuselage

Research found that the advantages of the high wing greatly outweighed the advantages of the low wing. Such advantages included better stability, ease of construction, and that the high wing would not take up any of the room in the fuselage. It was also determined that if a desirable aspect ratio was to be used on the wing, the 5 ft. wing span would not produce enough lift for the estimated weight of the aircraft. A decision to utilize a folding wing was therefore made. Other findings showed that although the circular fuselage would slightly reduce the drag of the aircraft, the difficulties of its construction would drastically increase its cost. It was also found that much of the space in the circular fuselage could not be used. The rectangular fuselage was then presented as the best design choice. Our final design is presented in figure 4.

Scale 1" = 1'

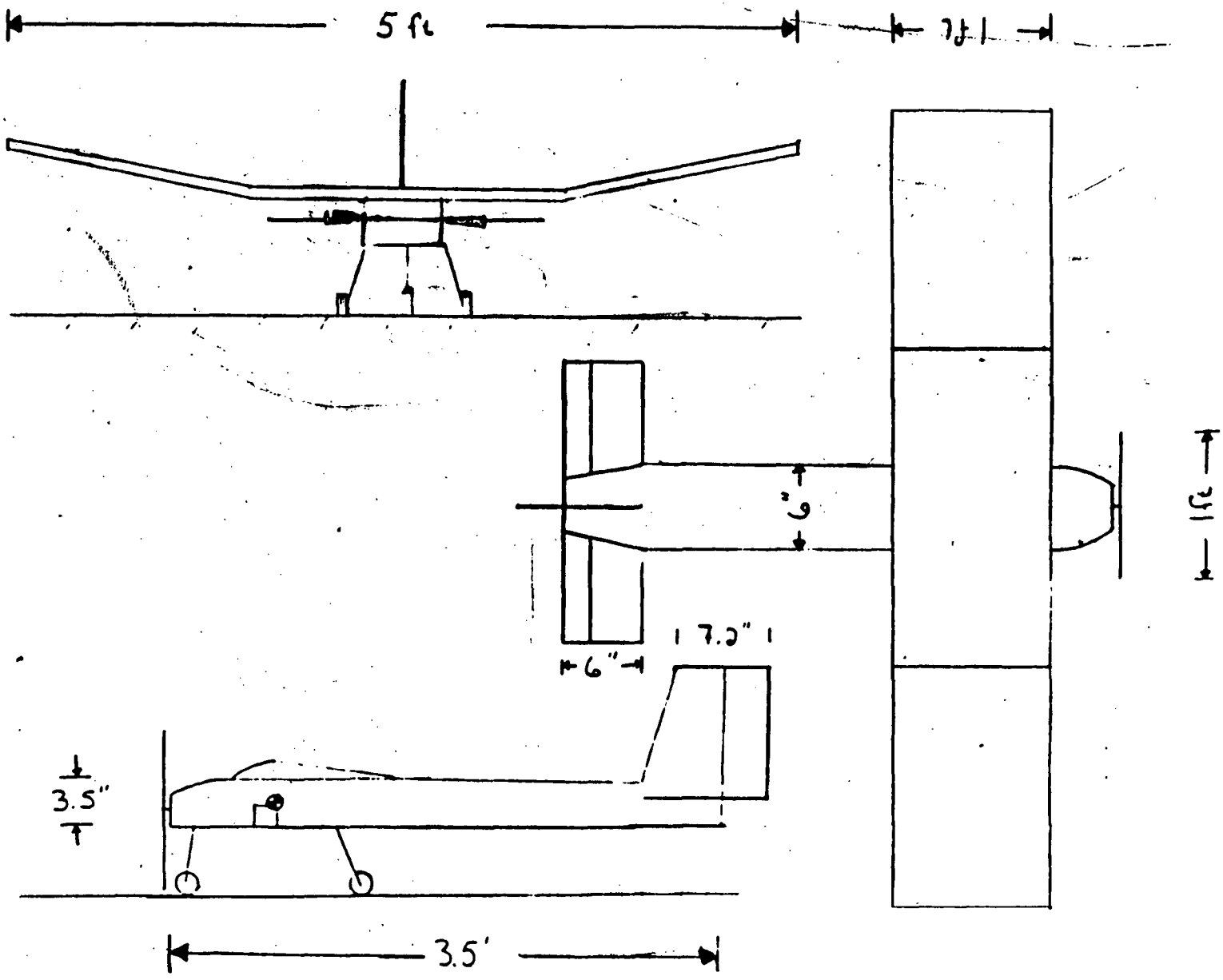

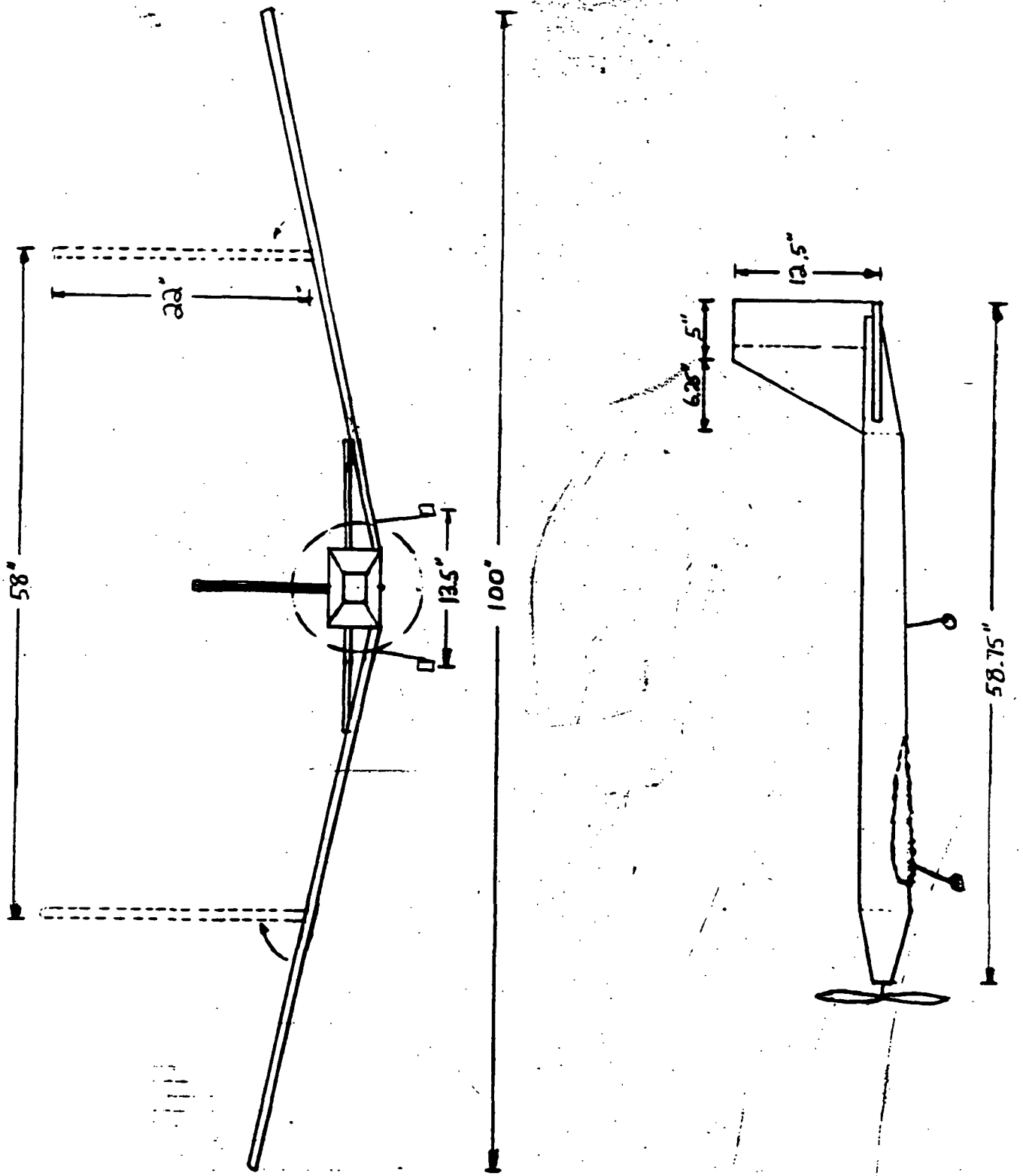

ENGR.			REVISED	DATE		
CHECK						
APR						
APR						
					BOEING	

LMB-1

"Fly By Night"

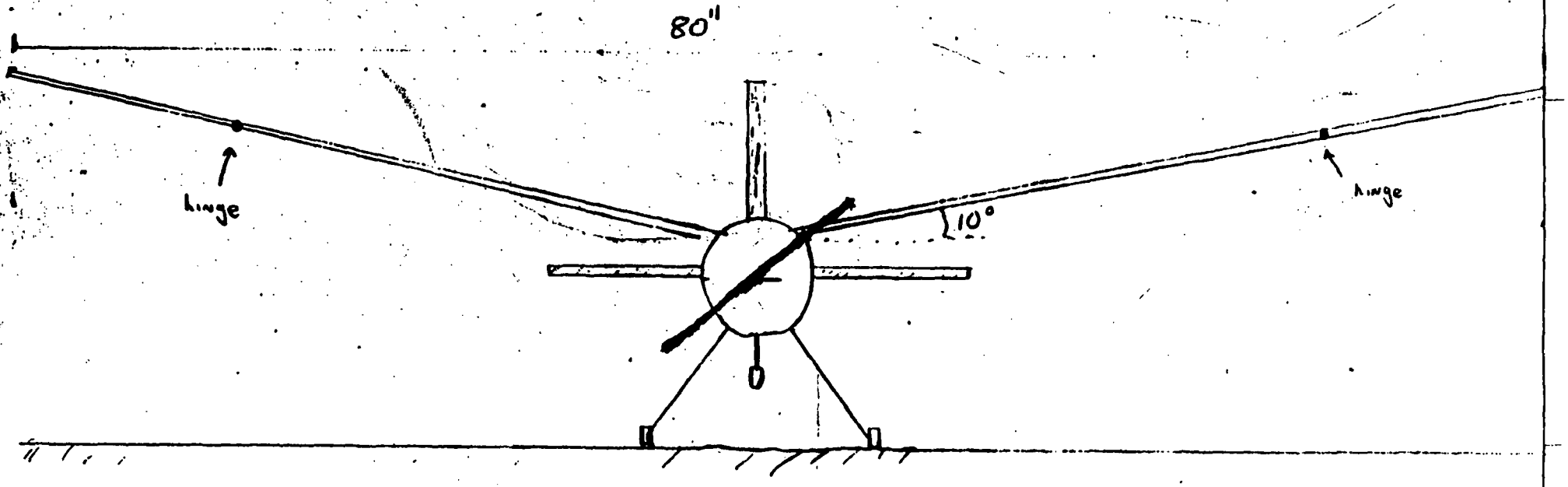

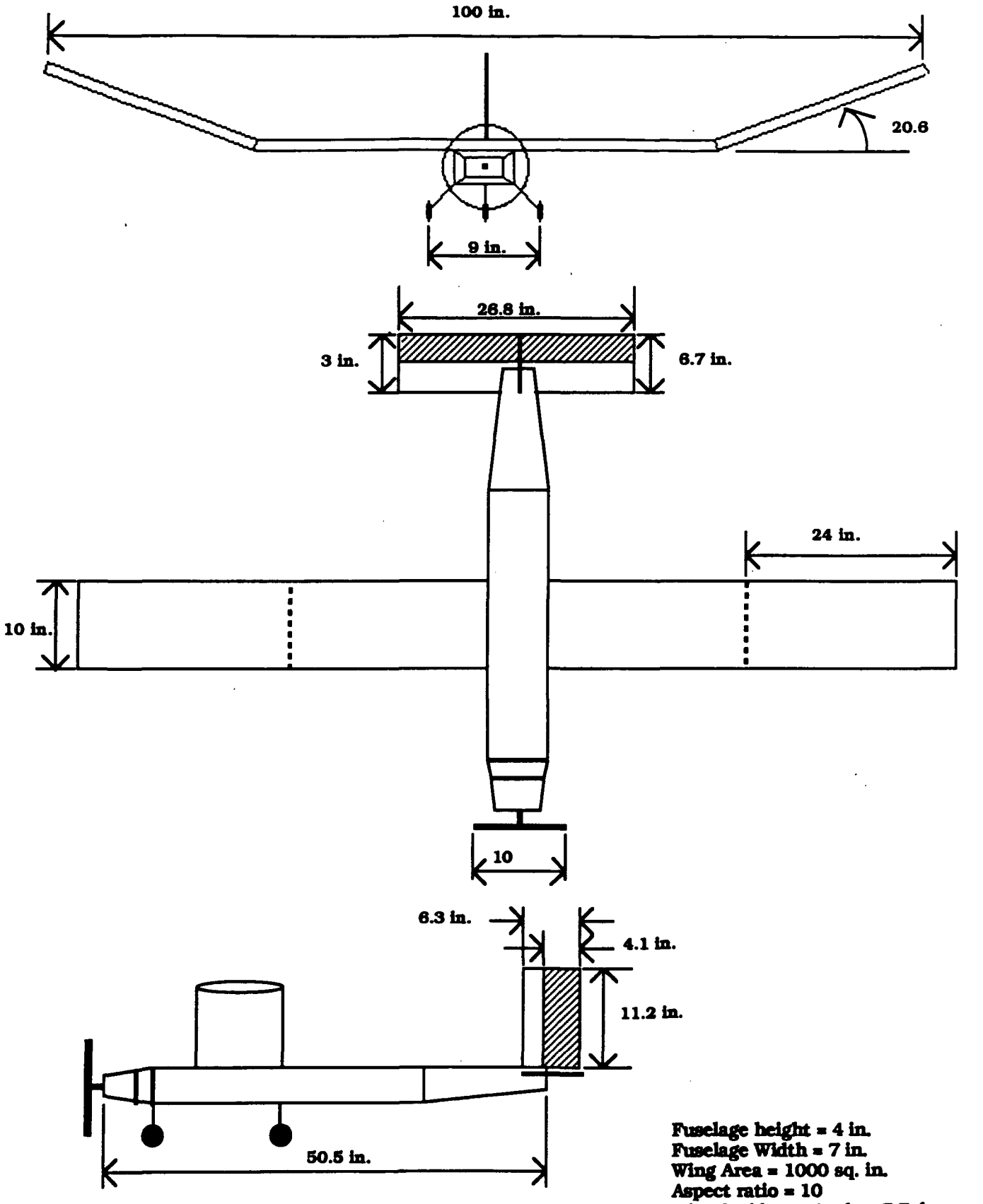

Fuselage height = 4 in.
Fuselage Width = 7 in.
Wing Area = 1000 sq. in.
Aspect ratio = 10
Wing Incidence Angle = 7.7 deg.
Weight = 80 oz.
Control : Rudder and Elevator
Engine : Astro Cobalt 15 - Geared
Propeller : Zinger 10-6

SCALE : 1 in. = 15 in.

D. AERODYNAMIC DESIGN

D.1 AIRFOIL SELECTION

The first objective of the aerodynamics group was to select an airfoil section. An initial estimate of the design Reynolds number (150,000) was made using our desired cruise velocity and a chord length of 1 ft. Thus, a primary constraint in the airfoil selection was to consider only airfoils which performed well at low Reynolds numbers (100,000 < Re < 200,000). A host of such airfoils were found in reference 5. In order to reduce the number of candidates several figures of merit were established.

Desirable airfoil characteristics included:

A high Cl_{max}

Good stall characteristics

Low costs and ease of construction

Durability

It was also determined from analytical analysis (equation 4.6, ref. 4) that the thickness to chord ratio of the airfoil needed to be less than 17%. At higher ratios the amount of zero lift drag, Cdo, increased dramatically as shown.

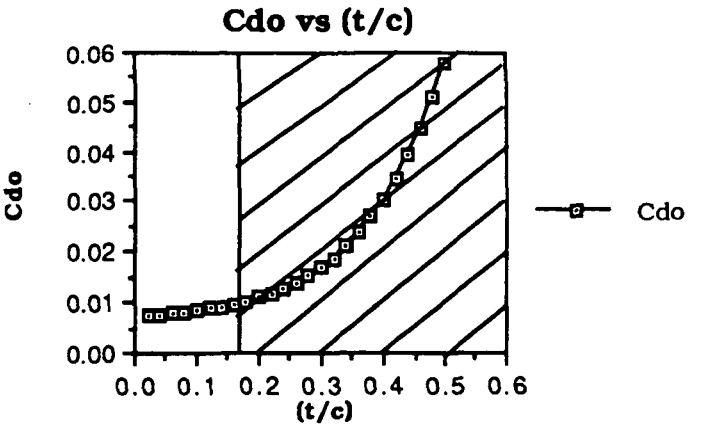

Figure D.1

Three airfoil shapes, the FX63-137, the Clark-Y, and the Spica, were chosen as candidates for our design. Although the FX63-137 has the greatest Cl_{max}, 1.6, its overall shape, with a thin trailing edge, posed problems for construction, therefore increasing construction costs. The thin trailing edge also posed durability problems when handling and transportation of the wing were considered. Although the Clark-Y had a much better shape in terms of construction and durability in comparison to the FX63-137, it had the lowest Cl_{max} of the three competitors, Cl_{max} of 1.2 in comparison to a Cl_{max} of 1.4 for the Spica airfoil. The Spica also exhibited a much gentler stall behavior in comparison to the other candidates which, when combined with its high Cl_{max} enables it to perform the tight turns necessary for the successful completion of our mission. The Spica airfoil also met the construction and durability requirements with its simple flat bottom shape. Selection of the Spica airfoil was therefore made.

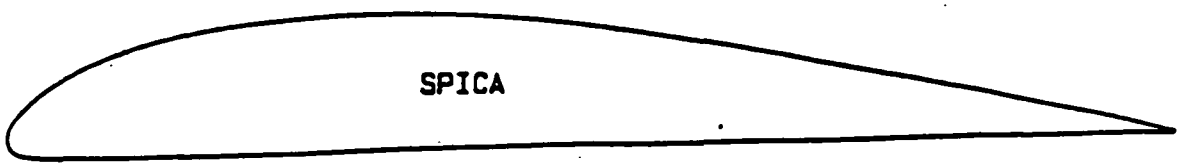

Thickness 11.72% Camber 4.74%

Figure D.2

D.2 WING DESIGN

With the selection of the airfoil section complete it was now necessary to determine the size of the wing for our airplane. First, corrections of the airfoil data for the effects of a finite wing were made. The lift-curve slope was corrected using equation 5.53 of reference 1.

$$a_0 = \frac{a_0}{1+57.3\, a_0/\pi AR e}$$

This gave a lift curve slope of .075/deg. and a Cl_{max} of 1.196.

Parameters which we had control over were the planform area, the wing's aspect ratio , wing taper and wing sweep. In order to maintain simple wing construction it was decided that there would be no taper of the wing. At such a slow cruise speed, 28 ft/s, it was determined that wing sweep would be detrimental to our design. Wing sweep would reduce the effective velocity of air on the wing, reducing the Reynolds number which would increase drag. Studies of the effect of varying the other parameters showed the following results.

The induced drag or drag due to lift, Cdl, was calculated for various aspect ratios for given planform areas using equation 4.8 ref 4, in conjunction with equation 3.2.9 ref 2 to correct for the change in the Oswald efficiency factor with changing aspect ratios. These results

were then graphed and it was clearly visible that increasing the aspect ratio significantly reduces the amount of induced drag. It is also apparent that for a given aspect ratio, induced drag is reduced as the planform area is increased. However, it should be evident that as the size of the wing is increased, the weight of the wing also increases.

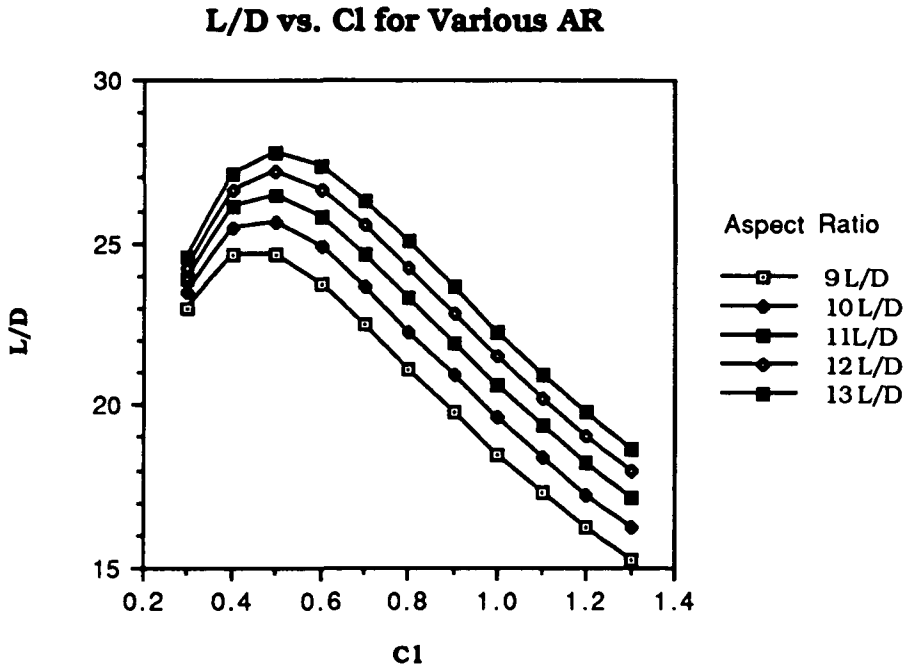

Figure D.3

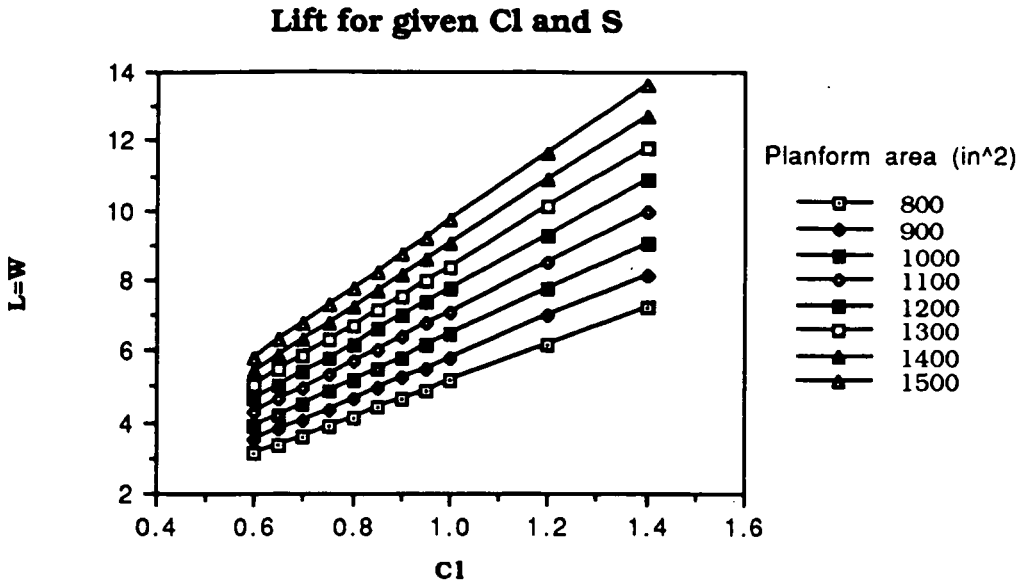

Figure D.4

Figure D.3, a graph of L/D at various CLs and various aspect ratios shows that as the aspect ratio is increased the L/D ratio at a given CL also increases. We also see that L/D max occurs at a CL=.5 and L/D decreases with increasing CL. Using figure D.4, the lift for a given CL and planform area in conjunction with figure D.3 we find, as we should expect, that a lower lift coefficient is needed for an airplane of a given weight when the planform area is increased. This reduction in CL required gives an increase in our L/D performance. Total wing drag, C_D, vs aspect ratio (figure D.5) shows the benefit of drag reduction associated with increasing the aspect ratio.

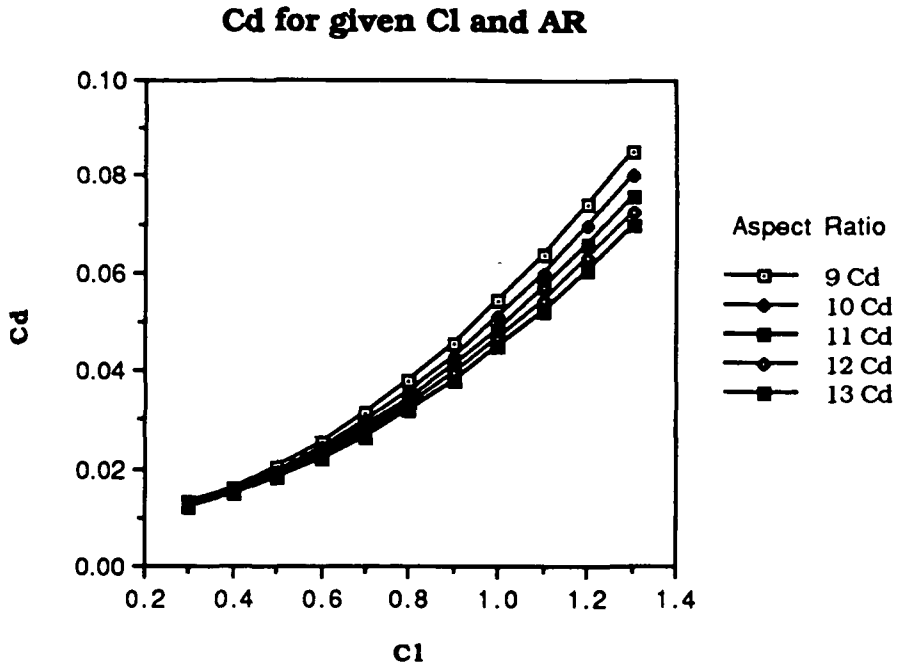

Figure D.5

The wing planform area and aspect ratio were chosen for this aircraft in order to optimize cruise performance while taking into consideration structural limitations placed on the wing. Figure D.6 shows the performance of a five pound airplane (the design weight) in cruise at Mach 0.8 (28 ft / s, the design cruise velocity). Power required, and hence range and endurance, are plotted versus wing area for various aspect ratios. This plot shows that aspect ratio has more of an influence on power required than does wing area, and that a high aspect ratio is desired to reduce the power required, thus increasing range and endurance.

Several other design goals and requirements are overlaid on this plot in order to narrow the range of possibilities for the wing design. From a "rule of thumb" analysis it is determined that the wing loading for an aircraft of this type should be between 0.6 and 1.0 lbs / ft^2. This places an upper limit on wing area. The takeoff velocity should

not be greater than the cruise velocity - this places a lower limit on wing area. The coefficient of lift for cruise may not be greater than Cl max - all values satisfy this requirement. These aerodynamic and performance requirements place limits on the wing area but do not restrict aspect ratio. Thus it would seem that any aspect ratio may be selected, the higher the better. However, after conferring with the structures group, a final limit is placed on the graph so that an all balsa wood wing will be able to withstand the stresses at the root chord (with appropriate safety factors). From this graph the design point is selected to be a wing area of 1000 in^2 and an aspect ratio of 10.

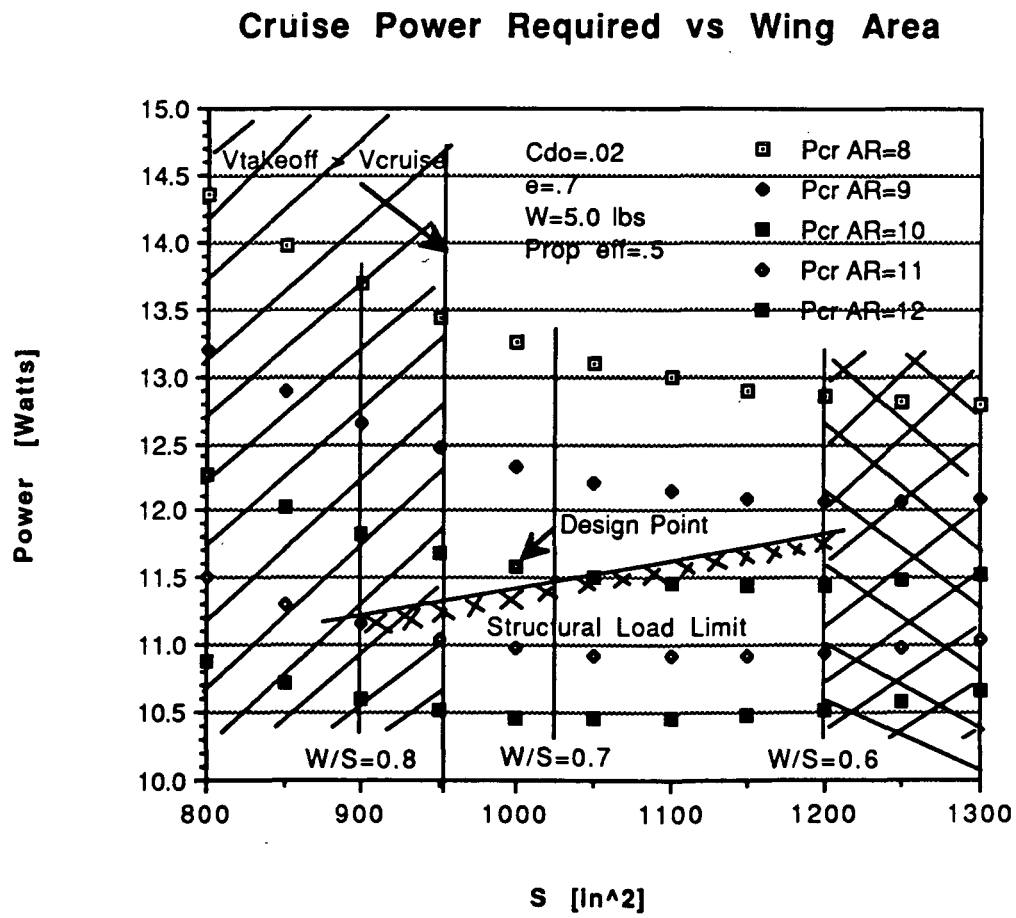

Figure D.6

Some assumptions had to be made in the study of the wing drag and performance calculations. For example, some of the data used was extrapolated from graphs which did not give results in the range of Reynolds numbers in which we were operating (Figure 4.3, page 25, ref 4). Some equations used were formulated from a broad range of previous data and were not derived from basic principles (such as equation 3.2.9 ref. 2). This is further explained in the references near any equations for which this feature applies. All calculations were made for the wing alone, meaning that no account was made for the interference associated with mounting the wing onto the plane. C_{Do}, C_D and Cdl are for the wing alone and not for the entire aircraft.

D.3 FUSELAGE DESIGN

The goal of the aerodynamics group in designing the fuselage was to reduce the drag as much as possible. However, it was found that very few changes in the fuselage design could be made due to the required passenger area of the fuselage, and design requirements limited the overall size of the fuselage. This, in turn, limited the minimization of the fuselage drag to the design of the nose and tail sections. For information on the equations utilized and associated information see Ref. 3.

Because of the location of the engine, alterations of the nose section were fairly restricted. The effect of the nose section on drag can be seen in figure D.7 below. From this data we see that a longer nose is desirable. However, this graph does not tell the complete story for from figure D.8, we see that a longer nose creates a longer

fuselage thus increasing drag. An optimum nose length was determined to be 5.5 inches with a vertical taper angle of 7.5 degrees. The horizontal taper of the nose was made to decrease the frontal area and thus drag, resulting in 2 inches with 8 degrees taper followed by an additional 3.5 inches tapered an additional 8 degrees.

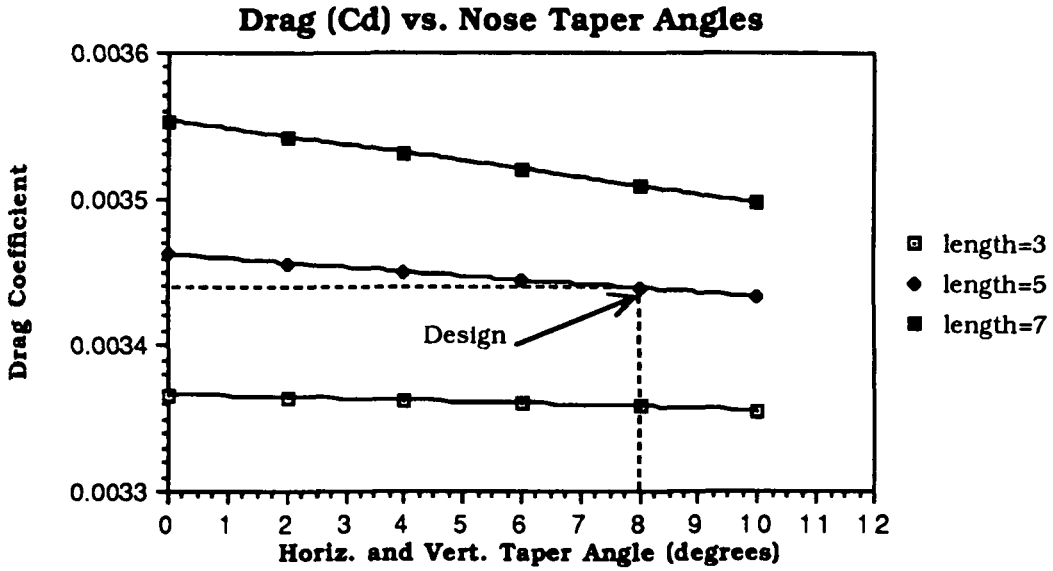

Figure D.7

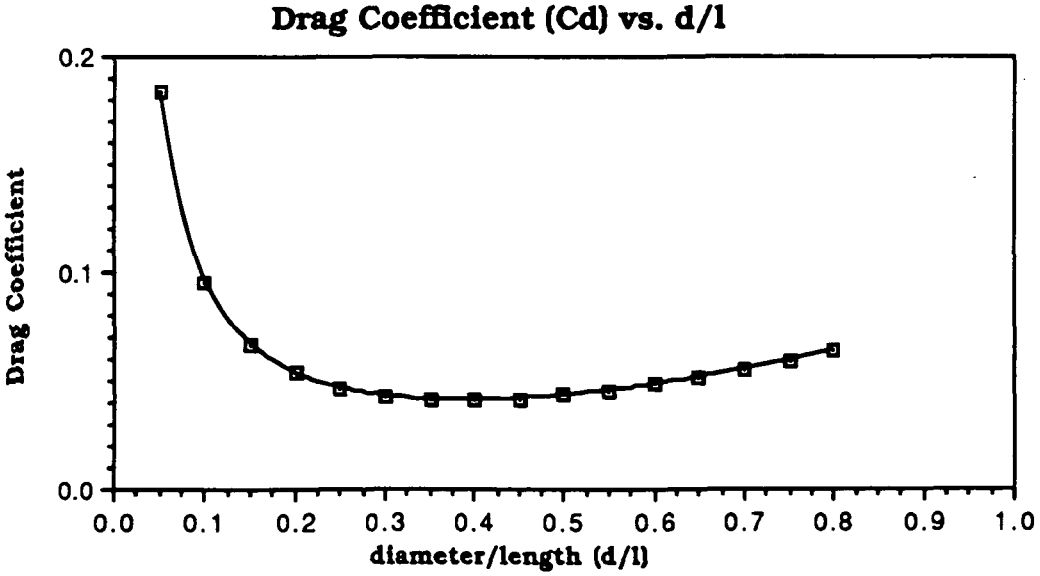

Figure D.8

In designing the tail section it was found that a boat tail construction would be the most beneficial design for this project. This allowed for ease of construction and placement of the control systems. Based on the effects of boattail angle (Figure D.9), an upsweep angle of 6 degrees was selected for the tail because any further increase in upsweep lead to an increase in drag due to flow separation. The length of the tail was determined to be 14 inches. This was determined by several factors. First, with an upsweep of 6 degrees a short tail would lead to a large base area at the rear which creates a pressure drag. However, increasing fuselage length also increases drag as was shown in figure D.7. An optimum design of 14 inches was thus selected. Also considered in the design of the tail section is the effects of the tail horizontal taper angle on the drag coefficient. From Figure D.10 it is evident that as taper angle increased, the drag coefficient decreased because of the lower wetted surface area resulting from taper.

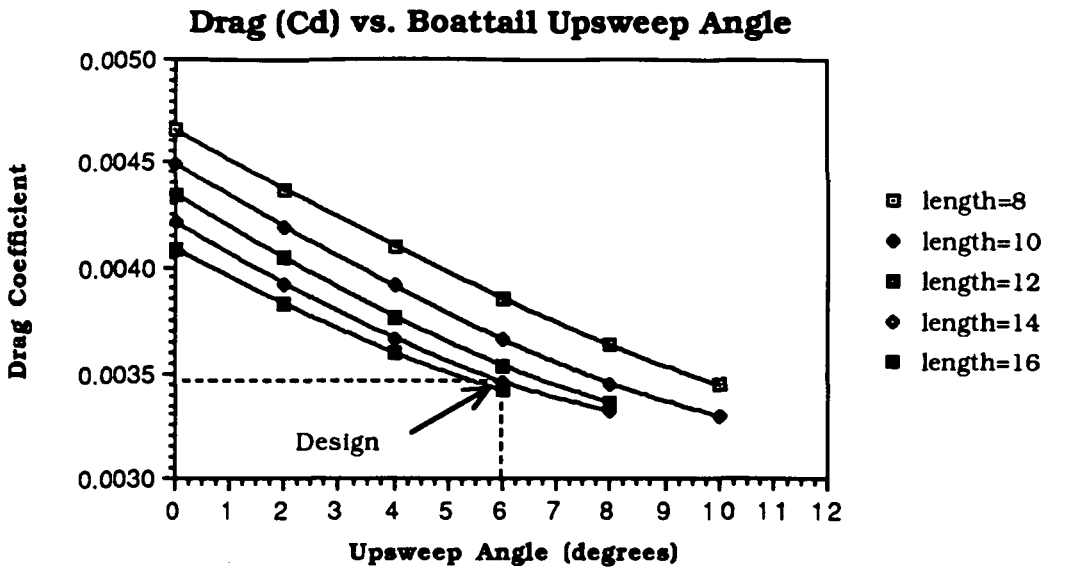

Figure D.9

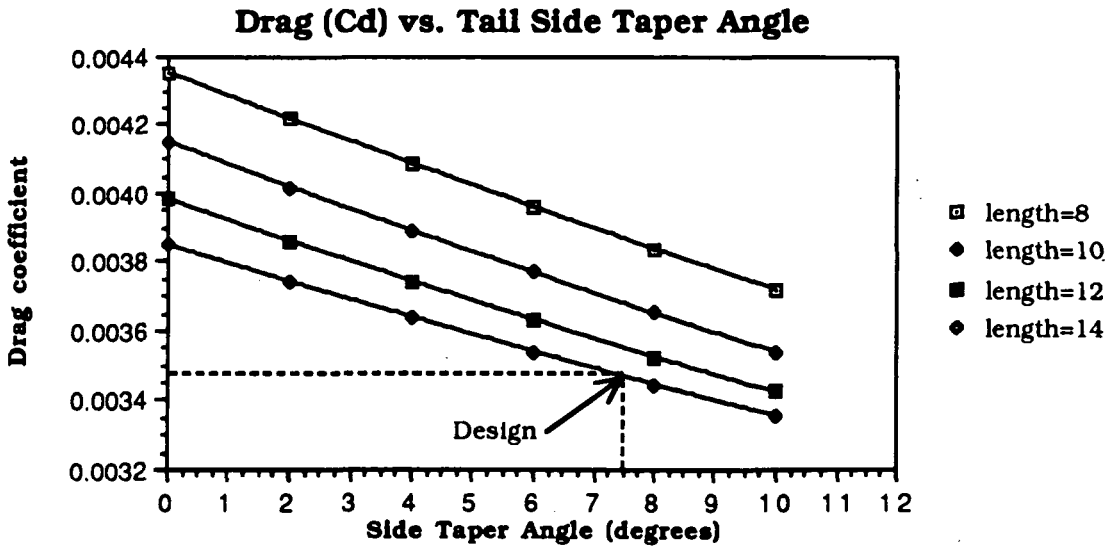

Figure D.10

D.4 DRAG PREDICTION

Estimates of the aircraft drag were made through the use of the drag breakdown method (ref 3). First an estimation of the parasitic drag was made using the following equation

$$C_{Do}=\frac{1}{S_{ref}}\Sigma C_{Doi}A_i$$

C_{Doi}-component drag coefficient

A_i-area on which C_{Di} is based

The C_{Doi} of the wing was determined analytically using equation 4.6, ref 4. while the fuselage C_{Doi} was determined by equation ref 4. Other contributions were estimated from typical values given in reference 2 & 3.

Component	CDoiAi/Sref
Wing	.009
Fuselage	.003
Horizontal Tail	.00128
Vertical Tail	.00056
Landing Gear	.000675
Interference	Add 5% to CDo
Roughness and Proturberances	Add 10% to CDo
Total Plane CDo	.0167

Using a safety factor of 1.20 we thus arrived at an airplane CDo = .020

The induced drag or drag due to lift, C_{Dl} was also calculated using the equation

$$C_{Dl}=\frac{C_L^2}{\pi ARe}$$

With this equation it was necessary to calculate the Oswald efficiency factor,e, for the entire airplane. This was done with the following equation

$$1/e=1/e_{wing}+1/e_{fus}+1/e_{other}$$

The wing efficiency was calculated analytically.

$$e_{wing}=1.78(1-.045AR^{.68})-.64$$ (eq. 3.2.9, ref 2)

This produced a value of $e_{wing}=.757$.

The efficiency factor for the fuselage was estimated using figure 2-28 (ref 3).

insert graph

This gave a value of $1/e_{fus}$=.06 Finally, $1/e_{other}$ was estimated to be .05, a typical estimate given in ref 3. The total Oswald efficiency factor for the entire plane was then calculated and was found to be, e=.7.

With this information the planes Drag vs CL could be determined and plotted

$$CD=CD0+\frac{CL^2}{\pi ARe}$$

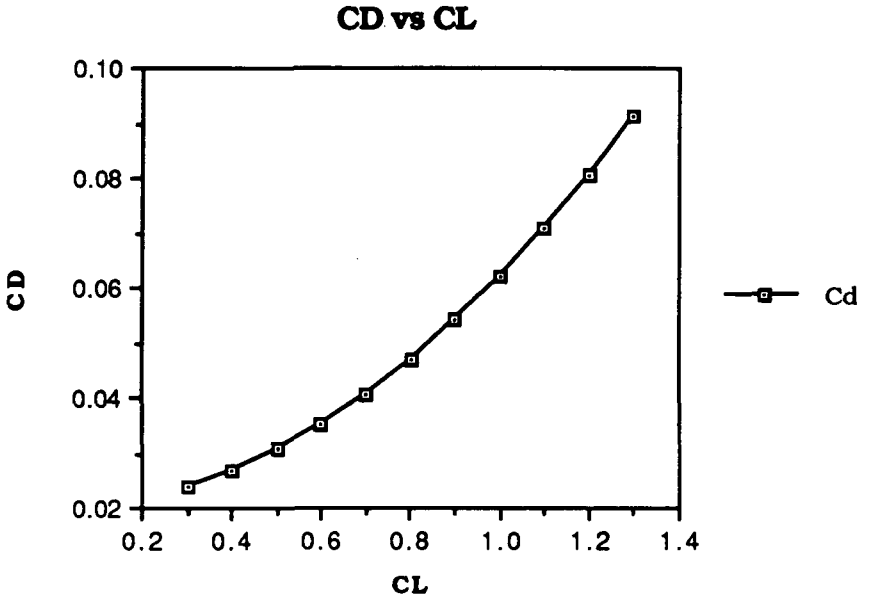

Figure D.11

D.5 AIRCRAFT AERODYNAMIC SUMMARY

Airfoil	Spica
CLmax	1.196
CDo	.020
AR	10
e	.7
L/Dmax	17.24
L/Dcruise	17.11
$\tau\ (\frac{c_{root}}{c_{tip}})$	1
Λ sweep	0

AERODYNAMIC SUMMARY GRAPHS

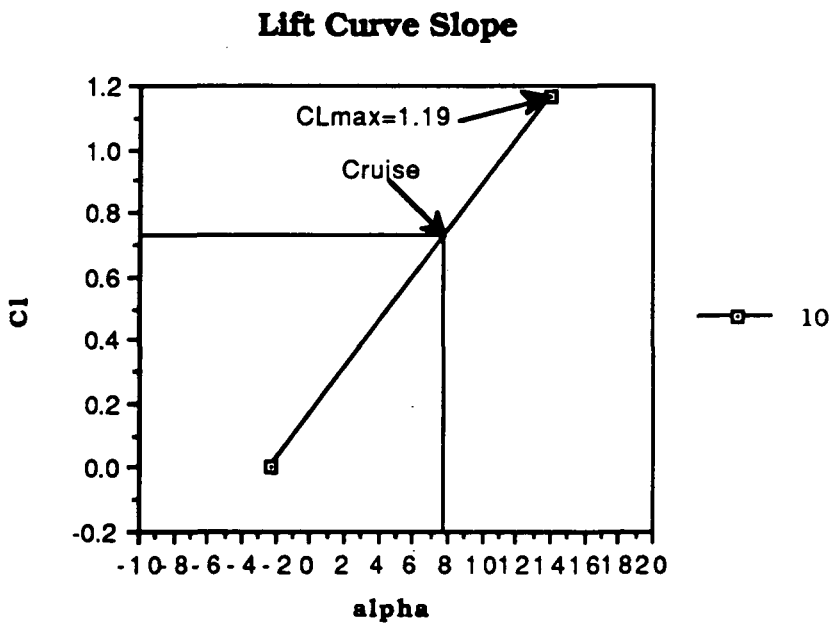

Figure D.12 Aircraft Lift Curve Slope

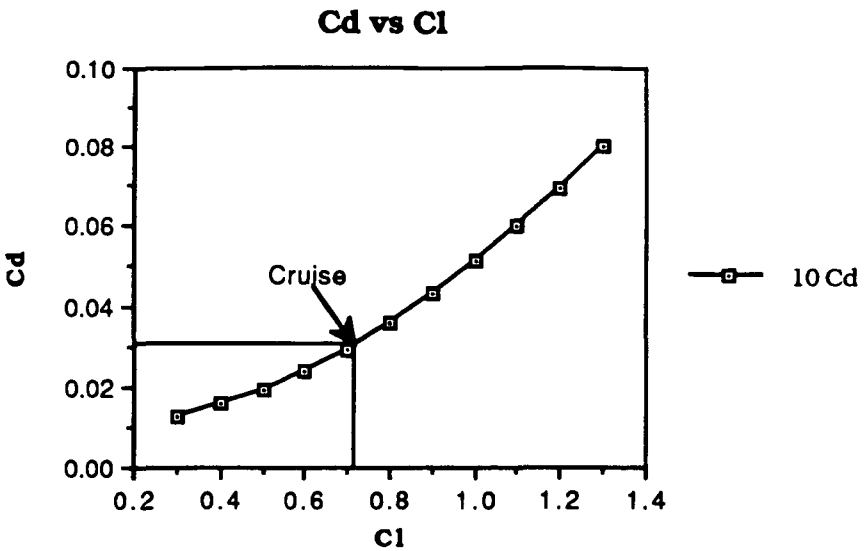

Figure D.13 Airplane Drag Polar

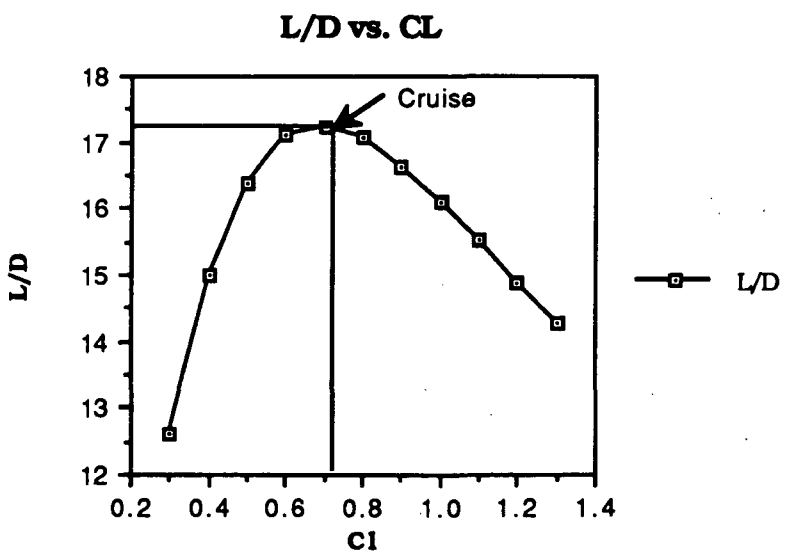

Figure D.14 Airplane Lift to Drag Ratio at Various Cl

E. PROPULSION SYSTEM

E.1 SYSTEM SELECTION

Mission specifications given in [3] reduced the number of propulsion system design options that could be considered for this RPV. First, the aircraft had to be able to take off and land under its own power. Additionally, the RPV had to be electrically powered and the engine choice was restricted to a group of engines recommended by the instructor. Lastly, the aircraft had to be controlled with a Futaba 6FG radio system. For these reasons, the procedure to select the characteristics of the system was quite short.

One important decision that was made in the initial phase of the design process was that only one engine would be used. More than one engine was assumed to be impractical mostly because Beta Systems wished to minimize the weight of the aircraft rather than produce the power to lift a heavier RPV. Another consideration was the fact that the two engines would probably have to be mounted on the wings. From a structural viewpoint, this idea did not seem wise. Two engines would be safer during flights over water, but as one member of the design group has so eloquently stated: "We're not worried - ping pong balls float."

E.2 ENGINE SELECTION

From the beginning, the propulsion design team saw that it would be necessary to choose the engine type based on the amount of power required at takeoff since the RPV has to be able to takeoff and land under its own power. With this design requirement in mind, the power required for the takeoff phase was found with the following equation from [2]:

$$P_o = W \left\{ \frac{1.44\,[W/S]}{\rho g C_{L_{max}} X_{GR}} + \mu \right\} V \qquad \text{(E.2.1)}$$

From preliminary investigation, the propulsion team found that the most uncertain variable in Equation E.2.1 is the ground roll friction coefficient. Using Figure E.2.1, the team was able to predict what effect a change in this parameter would have on the takeoff performance of the RPV.

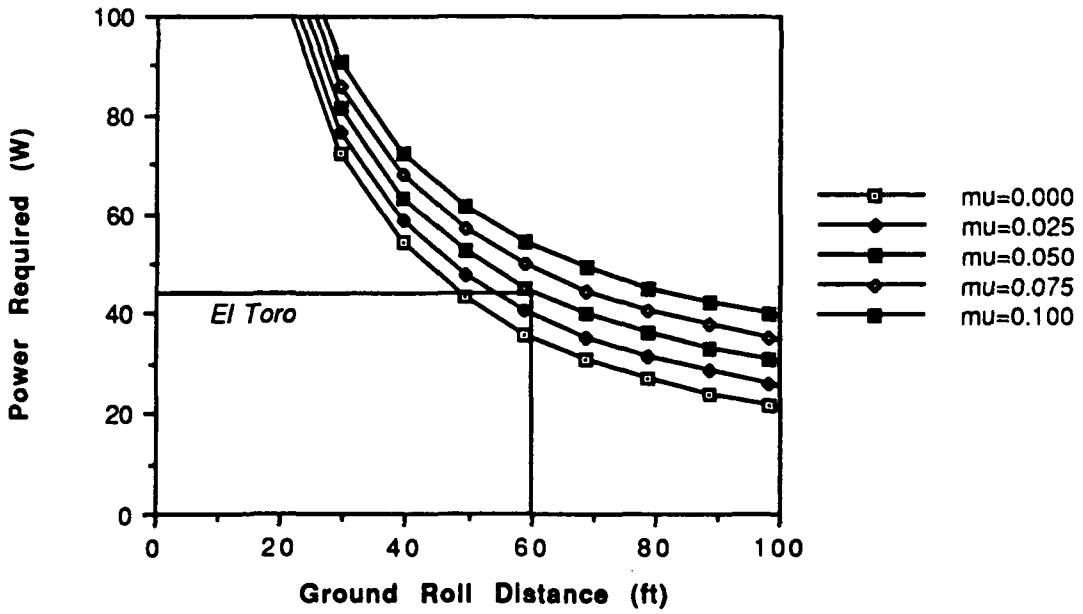

Figure E.1. Power Required vs Ground Roll Distance (Takeoff).

One should note that a 50% increase in μ results in a 30% increase in the takeoff power required for the same distance. Obviously, any difference in the ground roll friction coefficient would significantly change the takeoff performance.

Once the power required was found for takeoff, an evaluation of the power required for steady, level flight was conducted. A trade study was conducted on the effects of different aerodynamic parameters on the power and the propulsion team concluded that of all of the variables involved in the expression below (see [1]), the parasite drag coefficient most effects the amount of power required at cruise.

$$P_{REQ} = \frac{1}{2} \rho V^3 S \{C_{do} + \frac{C_L^2}{\pi e AR}\} \qquad \text{(E.2.2)}$$

Figure E.2 verifies this prediction.

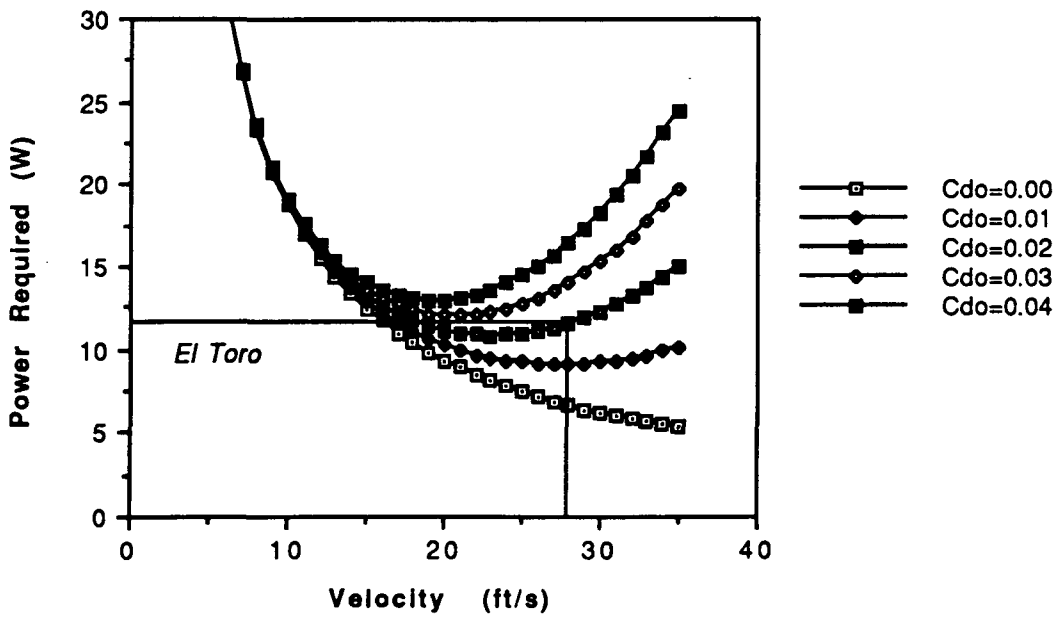

Figure E.2. Power Required vs Velocity (Steady, Level Flight).

In the course of the design process, the aerodynamic team found that its original estimate of C_{do} (0.045) was extremely pessimistic and that, in fact, the parasite drag coefficient is 0.02. Thus, the power required to takeoff was reduced by nearly 50% from the original estimated value.

One of the major deadlines in the propulsion system design was the engine selection deadline. Because the propulsion team was working with rough aerodynamic parameters in the weeks before that deadline, the amount of power required at takeoff and for cruise were much higher than the final values. For example, the original belief of the propulsion team was that 60 W would be required to lift the RPV off the ground. This assumption, however, was based on the ideas that the aircraft would be 6 lb and have a 1200 in^2 planform area. Assuming that a propeller would operate on any of the available motor types with an efficiency of 50%, the engine power was roughly determined for each engine as shown in Table E.1.

Table E.1. Engine Power for Available Engines

(50% Propeller Efficiency)

Motor Type	NiCad Bat Pack	Pshaft	Pavail
Astro-020	4X800 mAhr	50 W	25 W
Astro-035	5X800 mAhr	90 W	45 W
Astro-050	7X900 mAhr	125 W	63 W
Astro-150	12X900 mAhr	250 W	125 W

From this analysis the Astro-020 and Astro-035 were rejected because they did not provide enough power. The Astro-05, meanwhile,

provided enough power but did not appear to have any safety room for operation. For these reasons, the Astro-15 was chosen as the motor for *El Toro* when the deadline for engine selection arrived. It is important to be aware that the motor used in this system will be a geared model and will allow the propeller to turn with a different RPM than the armature in the engine. The gear ratio for the Astro-15 is 2.214.

Subsequent calculations (for a 5 lb, 1000 in^2 of wing aircraft) have revealed that the RPV will takeoff with only 42 W of power produced by the engine. Likewise, the reduction in the parasite drag coefficient has lowered the required cruise power from approximately 25 W to 12 W. Beta Systems' *El Toro* will be powered by the Astro-15 Cobalt motor, but further derivatives may be able to use the Astro-05 Cobalt engine.

E.3 PROPELLER SELECTION

The selection of the propeller was intimately connected with the decisions concerning the operation of the engine type once it was chosen. The thrust and power produced by the engine is directly related to the propeller that is attached to it. For this reason, the best choice for a propeller would be the one which operates with the best efficiency over the widest range of power settings (and, thus, RPMs). The propeller for this RPV needed to have a diameter less than or equal to 12 inches because of the landing gear placement. The graphs of propeller efficiency versus advance ratio for three propeller types have been given in [4] and were used for this study. Using the cruise

velocity of 28 ft/s and the appropriate diameters of the propellers, the advance ratio was transformed into RPM and the efficiencies for the TopFlight 9-4, Zinger 10-6, and AirScrew 12-6 were examined over the range of RPV operation RPMs. Figure E.3 illustrates this relationship.

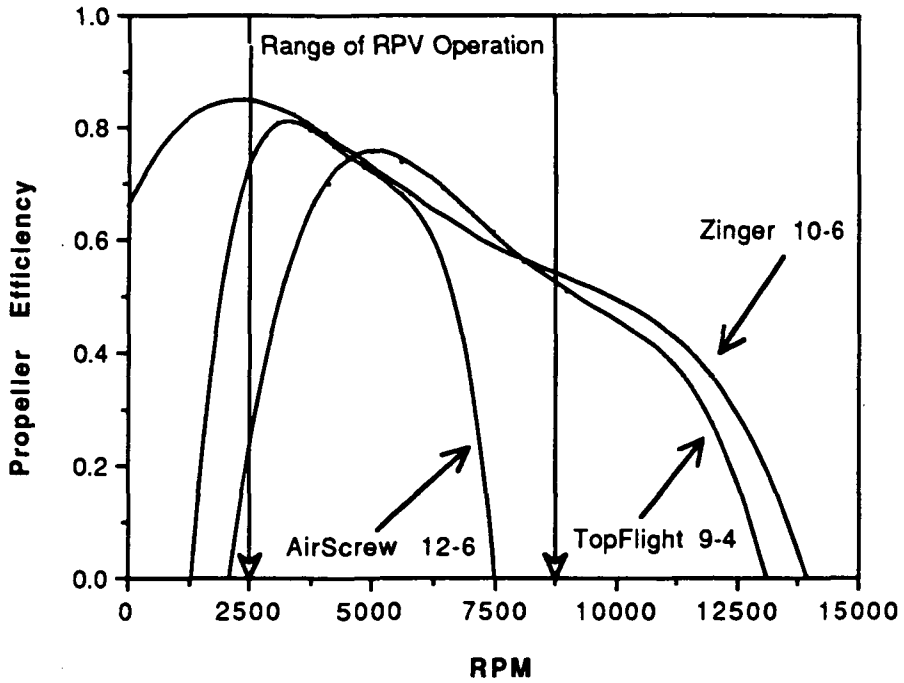

Figure E.3. Propeller Efficiency vs RPM (Zinger 10-6).

One should notice that the Zinger 10-6 performs better than the other two propellers over the operating range and therefore satisfies the original requirement for the propeller tpye.

Using a computer code by Barry Young, the efficiency, thrust, and power coefficients were generated for the Zinger 10-6. Figure E.4 shows the relationship between efficiency and advance ratio.

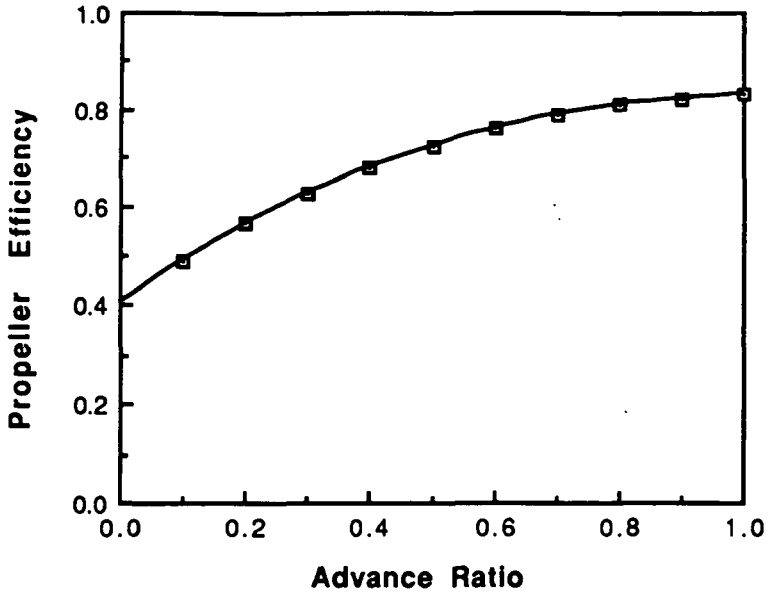

Figure E.4. Propeller Efficiency versus Advance Ratio (Zinger 10-6)

Values generated by the code were inserted into a TK Solver routine which was used to show the performance of a propulsion system with the Astro-15 engine and the Zinger 10-6 propeller. From this computer application, the system proved to be capable of providing the power and velocity neccessary for *El Toro's* operation.

E.4 BATTERY PACK SELECTION

The propulsion team's decisions concerning the battery pack were mostly related to the requirements due to the engine type. Additionally, however, one of the mission requirements is that maintenance on the battery pack (i.e. replacement) must take as little

time as possible. Both of these factors figured in the selection of the battery pack.

According to the takeoff application provided by the instructor, the voltage required for takeoff is approximately 15 V. Since the cells which are used for this type of mission are only 1.275 V each, it was evident to the propulsion team that the battery pack had to be wired in series to increase the total voltage of the system. Before the first takeoff, therefore, there will be approximately 15.3 V available to the engine.

Using another application provided by the instructor, the propulsion team found that higher battery capacities yield higher ranges. Since the cells mentioned previously are sold with different capacities, the optimum capacity had to be chosen. After a cost analysis was conducted by the economics team, the propulsion team decided that the 1200 mAhr battery would allow for more than one flight to be conducted with the same battery pack while providing the most current (Note: the results of this analysis may be found in Section K). The difference in weight between the 900 mAhr cell and 1200 mAhr cell is negligible.

After the battery pack was selected as the P-120 SCRP, the Panasonic Corporation informed the propulsion team that it no longer manufactures 1200 mAhr batteries. Instead, Panasonic informed Beta Systems that it produces a 1300 mAhr battery with the same weight as the old 1200 mAhr battery. Since there is no weight penalty for operating with the higher capacity battery, *El Toro* will carry a twelve (12) cell, P-130 SCRP battery pack.

E.5 ENGINE CONTROL

From the beginning of the design process it was evident that some sort of speed control would be necessary because of the difference in the amount of power required for takeoff and cruise. The propulsion team knew that the addition of an electronic device (i.e. a speed controller) into the propulsion system would allow the remote pilot to be able to change the amount of voltage supplied to the engine (and, thus, the motor RPM). In the past, some design groups have been hindered in their decision to use a speed controller because they do not have enough weight allotted for such an addition. Beta Systems, however, planned to use such a device from the beginning and made room for the additional weight.

Since the voltage required to produce the appropriate power for cruise is less than the voltage necessary at takeoff, the electronic speed controller will be used in the system as shown in Figure E.5.

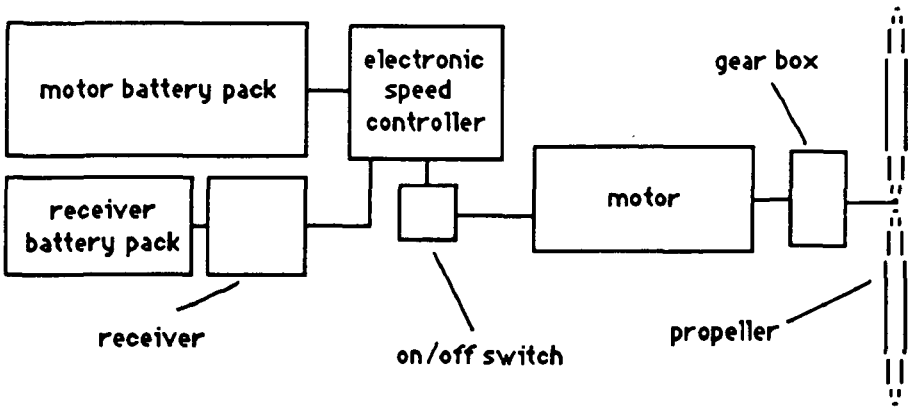

Figure E.5. Schematic Diagram of Propulsion System.

One should note that there will be a switch included in the system to prevent injury to anyone who is working on or near the propeller.

The speed controller will allow the remote pilot of the aircraft to change the voltage setting on the Futaba 6FG radio system and, thus, change the engine RPM. A change in the RPM, likewise, will change the amount of power available. *El Toro* will operate with an armature voltage setting of 8.05 V during cruise (as calculated with the TK Solver application) and with a setting of 15.3 V during the takeoff phase.

E.6 PERFORMANCE PREDICTIONS

If the system has been designed correctly, *El Toro* should be able to fly in steady, level flight as shown in Figure E.6.

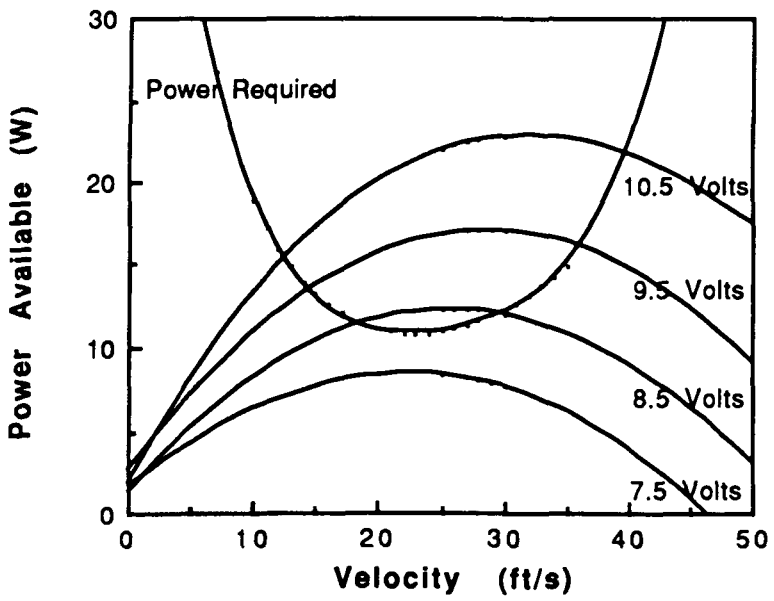

Figure E.6. Power Available for Different Voltages

Of course, the voltage supplied to the engine can be changed with the speed controller and more power will be available at higher RPM. *El Toro* will cruise with 12 W of available power, which corresponds roughly to a voltage setting of 8.05 Volts.

Comparing the performance of the RPV with the original mission requirements, the propulsion team was able to determine that *El Toro* can indeed takeoff and land under its own power, has an electric propulsion system, and can be controlled with the Futaba 6FG radio system. Further, the performance of the Astro-15 Cobalt motor with a Zinger 10-6 propeller was reviewed with applications provided by the instructor and proved to be a viable propulsion system. The current and voltage supplied by the P-130 SCRP battery pack has also been shown to meet mission objectives.

F. WEIGHT ESTIMATION

F.1 COMPONENT WEIGHTS ESTIMATION

In the design approach, initial weight estimates varied from 4-6 pounds due to uncertainty about fuselage size, structural weights, and propulsive performance. After deciding upon a payload capacity of 51 passengers, five pounds was agreed upon as the target weight. At the time, it was thought that this would be a low estimate for a plane of our size but it would still be attainable. Because the ensuing propulsion and performance calculations were performed using this estimate, it was decided to work towards this target rather than strive to find the absolute minimum weight possible. This decision allowed us to make conservative estimates so that we are more likely to be under our target weight, allowing us to carry the excess as additional payload, if necessary, for center of gravity manipulation.

The propulsion, fuel, avionics, payload, and propeller weights were accurately determined from available data following the selection of these systems. The difficulty was in estimating values for the other components; fuselage, wing, empennage, and landing gear. These component weights could not be accurately determined until the detailed structural design was completed, yet good approximations were necessary in order to locate the center of gravity for the tail sizings as well as to give the structures group some weight boundaries in forming the detailed design. It was presumed, however, that our plane would use similar materials and construction as the planes from former years; therefore, a data base was created of past planes'

structural component weights. The fuselage weight per unit volume and wing weight per unit area were collected for a number of past planes. Models similar to the nature of our construction design were used to approximate our structural weights by assuming no changes in scale effects and using our fuselage volume and wing area to generate estimates.

A slightly conservative estimate was made in case unforeseen construction problems occurred. This conservatism in estimation was possible because some excess weight existed to buffer our weight estimates. Initial estimates made from the preliminary detailed structural design indicate that the actual fuselage weight will be approximately 12.5 ounces. The additional 2.5 ounces allotted to fuselage structure weight can be used as ballast (in the form of passenger luggage) or for other components which exceed their weights estimation.

The landing gear weight estimation was also rather conservative. The heaviest landing gear from the previous year was chosen because of its sturdiness. Because our plane was nearly double the weights of the previous year and because of the poor performance of previous landing gears, it was decided to allot a fair amount of weight for landing gear in exchange for the added safety. Similarly, the empennage weight could not be accurately estimated without knowing the tail sizings. The weight was estimated initially using an approximate area and it was found that it did not vary much with changes in size.

TABLE F.1 - Initial Component Weights and Weight Fractions

COMPONENT	Weight (oz)	Weight Fraction(%)
Fuel	24	30.0
Propulsion	11	13.8
Avionics	7.5	9.4
Payload	4.4	5.5
Propeller	0.5	0.6
Fuselage	14.5	18.1
Wing	12	15.0
Landing Gear	3.5	4.4
Empennage	2.5	3.1

Component Weight Breakdown

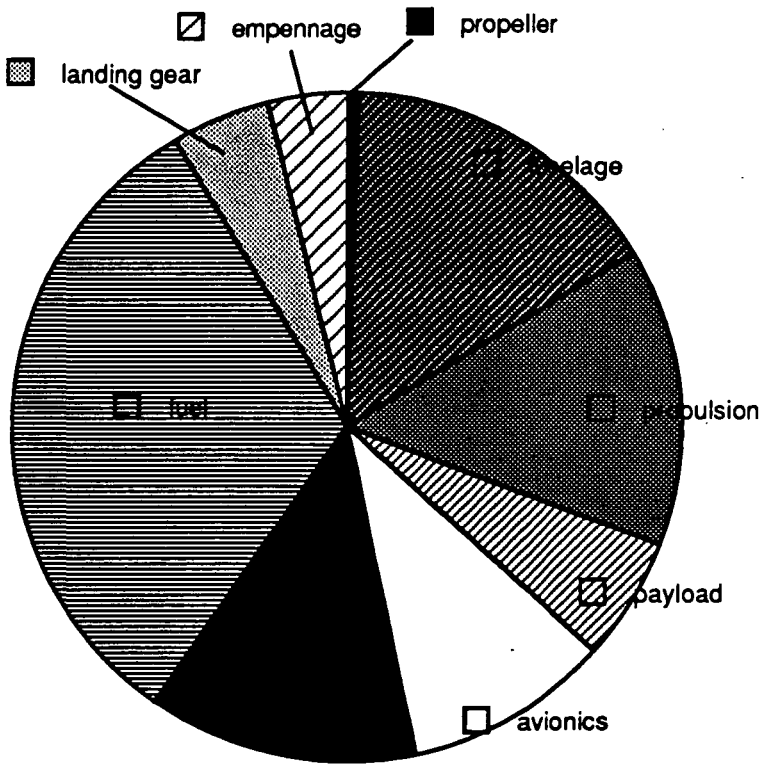

F.2 CENTER OF GRAVITY LOCATION

The determination of the center of gravity is paramount for the design of the airplane's stability control and ability to rotate at takeoff. To simplify the analysis, only the longitudinal center of gravity is considered important. This assumption is valid because the center of gravity of all components are designed to lie along the planform centerline. For longitudinal stability purposes the center of gravity is desired to be located as close as possible to the wing quarter-chord. The plane center of gravity is found from knowledge of the component weights and locations using the equation:

$$X_{c.g.} = \Sigma \ (X_{component} * W_{component}) \ / \ \Sigma \ W_{component}$$

The component weights and their x-locations are given in table W.2. The resulting x-location of the center of gravity is 13.67 inches from the nose of the plane. The wing quarter-chord is located 13 inches behind the nose of the aircraft for the fully loaded condition and 13.24 inches behind the nose of the plane for gross airplane weight without payload.

Table F.2 - Component Weights and X-Locations

COMPONENT	Weight (oz)	Distance from Nose (in)
Fuel	24	9
Propulsion	11	1.5
Avionics	7.5	12
Payload	4.4	21
Propeller	0.5	-2
Fuselage	14.5	22
Wing	12	15.5
Landing Gear	3.5	14.5
Empennage	2.5	49

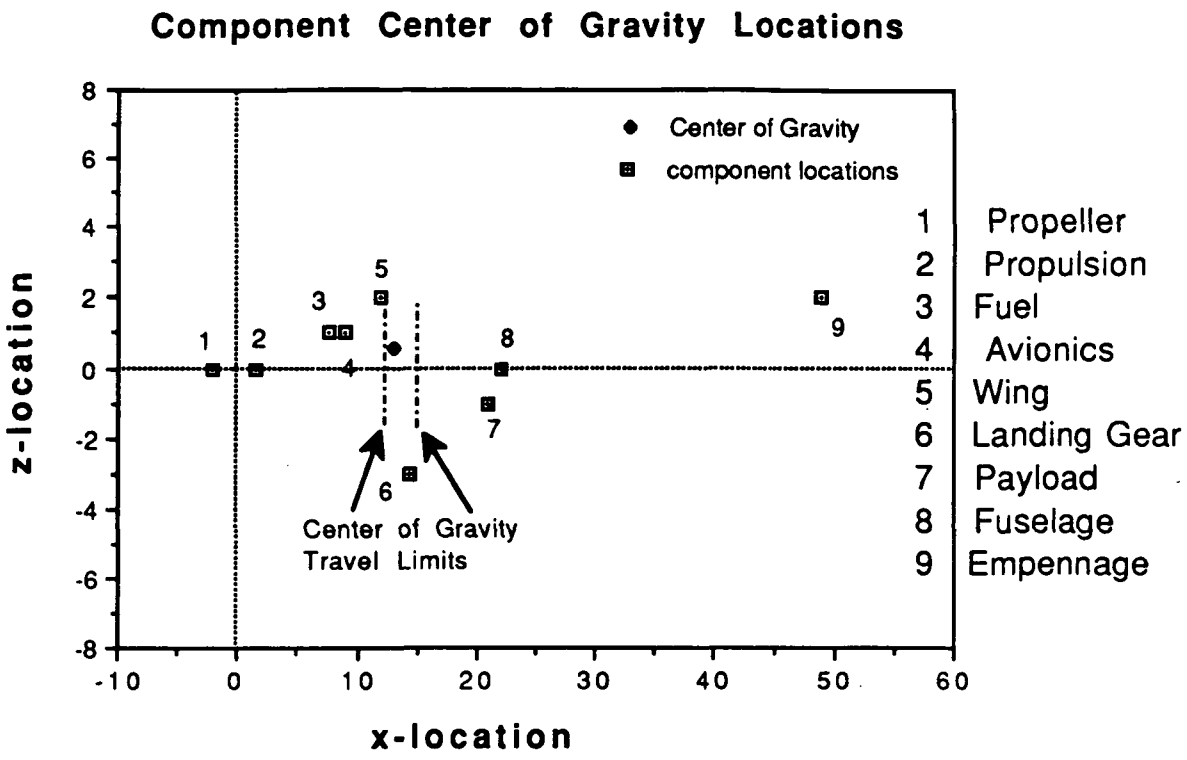

The proposed center of gravity locations provide suitable control for the aircraft by placing the center of gravity slightly behind the wing aerodynamic center. However, the estimation of both the weight and location of the fuselage as well as other possible weight errors introduces a considerable amount of uncertainty. In order to insure that the actual center of gravity is located in a favorable position, some measure of control must be implemented. The method for correction of error in fuselage and/or other estimation error is the internal placement of the fuel and control systems on the battery platform. If the center of gravity has to be moved forward, the fuel location can be moved forward, if it is too far forward and needs to be moved aft, additional available payload can be carried in the tail. This combination should allow sufficient control over the center of gravity position.

F.3 INTERNAL LAYOUT

The internal layout of the 'El Toro' is shown in Figure W.1. A platform has been used to mount the fuel and avionics package in the upper half of the first twelve inches of the fuselage section. This will allow easy access to the fuel by removing the wing. Refueling is the major contributor to groundtime and its reduction will save costs. Overhead mounting will also allow the control rods to extend in a straight line from the servos to the control surfaces. Otherwise additional structural loadings would be placed on the fuselage by mounting the control rods to the fuselage to bend the control rods.

The passengers will be seated three across with 17 rows for a total of 51 passengers. Each 1.5 inch diameter passenger will have a 2"x1.8"x1.75" space (the overhead space will increase to 4 inches behind the servo platform), which gives a payload volume per passenger 3.5 times larger than the passenger volume. Restrooms, galley, and additional baggage space will be available in the back of the plane. For the technology demonstrator, the passengers will be loaded either via the removed wing or through a hole in the fuselage skin. On an actual plane, doors would be placed under the wing and in the tail and the passengers would be able to load themselves.

The front section consists of a firewall to which will be connected the engine mount. Behind this firewall will be the speed controller followed by a second bulkhead to separate the payload compartment. This second wall will also help to reduce the vibration felt by the platform which could interfere with remote radio control.

Figure W.1: Internal Layout

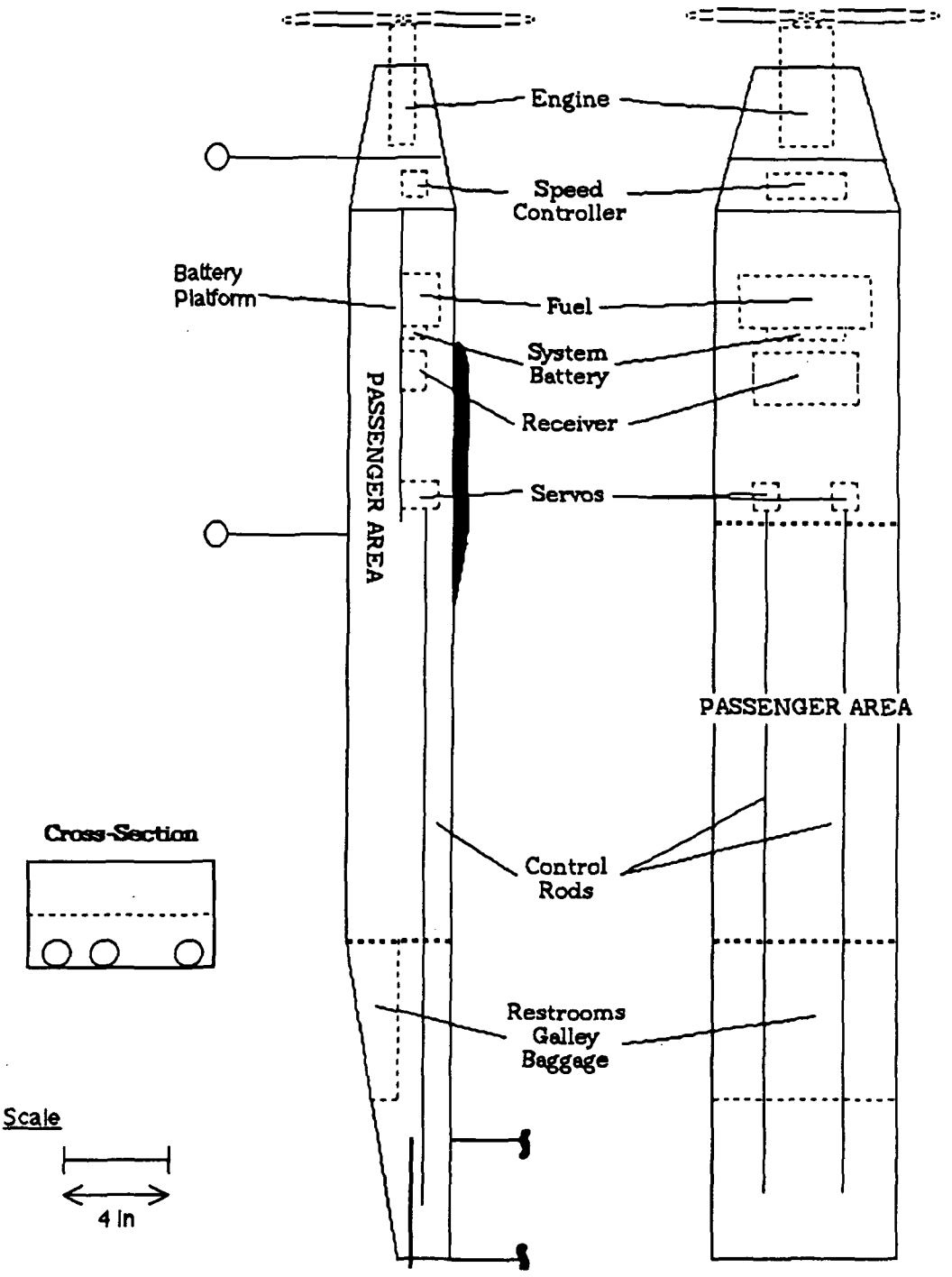

G. STABILITY AND CONTROL

The "El Toro" is a civil transport aircraft. For this reason, maximum passenger comfort and safety established a majority of the stability and control design requirements.

In designing a civil transport aircraft, Beta systems had one very large data base to go to for information, namely civil transport aircraft that we see every day. These aircraft led us to choose a conventional aft horizontal and vertical tail. This arrangement provides not only proven results but adds to passenger comfort. We feel that when passengers go to board an aircraft to which they are entrusting life and limb, they will prefer to board one that looks like a normal air transport.

G.1 LONGITUDINAL STABILITY AND CONTROL

Longitudinal Stability and control will be achieved with the horizontal tail with elevator. For our civil transport, maximizing stability is crucial. The 'El Toro" will not sell without insuring passenger comfort throughout the trip.

G.1.1 Static Margin and Center of Gravity Travel

In order to have a stable aircraft, theory states that the center of gravity must be forward of the neutral point. The neutral point is found by equation 1.

$$\frac{X_{np}}{c} = \frac{X_{ac}}{c} - \frac{Cm\alpha f}{Cl\alpha w} + \eta V_h \frac{Cl\alpha_t}{Cl\alpha_w}\left(1-\frac{d\varepsilon}{d\alpha}\right)$$

The "El Toro" has a neutral point at 61% of the mean chord. The static margin represents the distance of the center of gravity from the neutral point and is given by equation 2.

$$\text{Static Margin} = \frac{X_{np}}{c} - \frac{X_{cg}}{c}$$

For most aircraft, a static margin of at least 5% of the mean chord is desirable. However, the data base of Remotely Piloted Vehicles (RPV's) similar to ours and the advice of a model airplane expert dictate that the center of gravity be as close to the aerodynamic center as possible. Following this advice leads to a much higher static margin of 30%. The technology demonstrator will fly with its center of gravity at 30% of the mean chord giving a static margin of 30%. Figure G.1 investigates the effects of center of gravity travel on stability. The wing is mounted at a 7.7 degree angle of attack. Therefore the aircraft will cruise with a wing angle of attack of 7.7 degrees, or .134 radians.

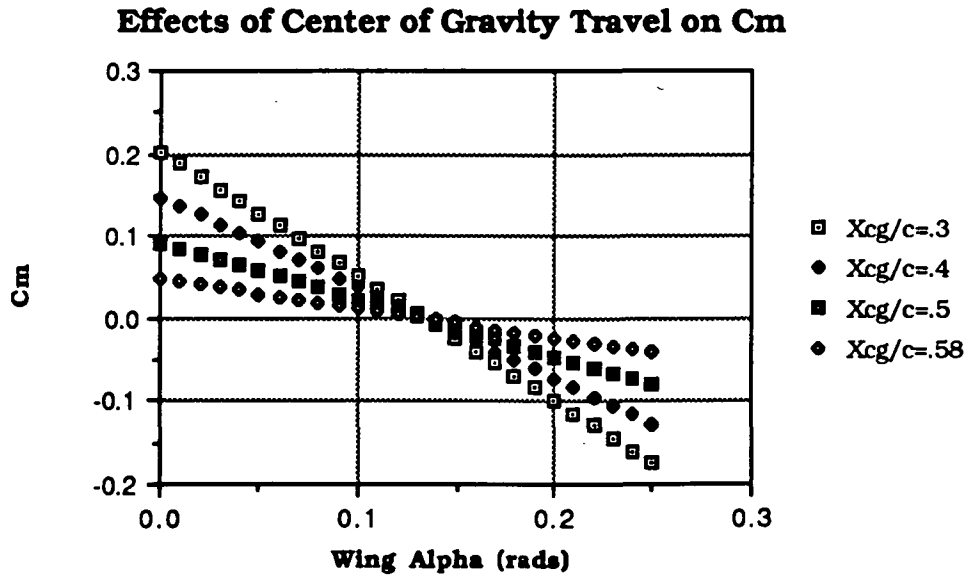

Figure G.1

Clearly, with the center of gravity at 30% of the mean chord, the aircraft will have adequate stability.

G.1.2 Horizontal Tail

In designing the horizontal tail of the "El Toro", the data base of RPV's from previous years and some standard rules of thumb (Ref. 3) controlled much of the early analysis. A small range of ideal volume ratio and tail aspect ratio values simplified the investigation. The design uses a median aspect ratio of 4 and a volume ratio of .65. Lower volume ratios were considered but .65 reduces the necessary tail incidence angle close to zero.

A flat plat airfoil section was used because of proven effectiveness in previous RPV's and ease of construction.

Calculation of the moment coefficient took into consideration mainly wing and tail components. Rough preliminary calculations of the fuselage contribution, using methods taken from Reference 1, showed negligible results for our design. The value of the moment coefficient is found using the relation

$$Cm_{cg} = Cm_o + Cm_\alpha \alpha$$

The "El Toro" has a Cm_o = .203 and a slope of -1.51. Again, for ideal values for the moment coefficient slope, previous RPV's as well as other sample aircraft were looked at. There is no guideline to how steep the moment slope must be. So, in order to insure "El Toro" could fly its passengers comfortably, typical slopes from previous RPV's were increased by 50% to give a range of values for our aircraft. Our moment coefficient slope falls within this range. The wing of the airplane is mounted at a 7.7 deg (.134 rads) angle relative to the

fuselage center line. This cruise angle of attack (assuming the aircraft will trim with no elevator deflection) and the moment slope gives the aircraft moment curve for cruise (Figure G.2).

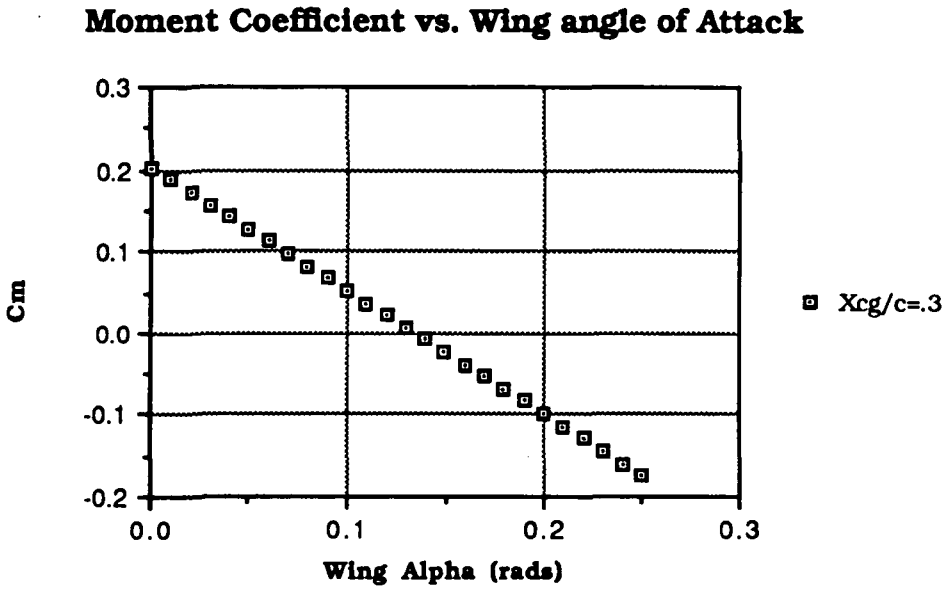

Figure G.2

G.1.3 Tail Incidence Angle

In order for our aircraft to trim at a wing angle of attack of 7.7 degrees, we must mount the horizontal tail at a positive angle of attack. The expression for the zero angle of attack moment coefficient is

$$Cm_o = Cm_{o_W} + Cm_{of} + \eta V_h \, Cl_{\alpha_t} (\varepsilon_o + i_w - i_t)$$

We obtained the value of Cm_o from Cm_α and the desired angle of trim. All of the other values, except i_t, are known from the airplane characteristics. This equation tells us that "El Toro" requires a 1.3

degree tail incidence angle for a trimmed condition at 7.7 degree wing angle of attack. Construction of trim tabs on the technology demonstrator would introduce too many problems but because good flying qualities are important, the tail incidence angle will trim the aircraft without elevator deflection.

G.1.4 Elevator

The elevator must provide sufficient change in moment coefficient in order to rotate the airplane at takeoff and to trim the aircraft at high angles of attack. The change in moment coefficient due to elevator deflection is

$$\Delta Cm = -\eta \, V_h \, Cl\alpha_t \, \tau \, \delta_e$$

The rear landing gear is located five inches behind the center of gravity. The gear placement at this location was driven by the need for clearance of the back end of the aircraft at takeoff. With a tricycle landing gear, the back end will dip down when the aircraft takes off. Movement of the rear landing gear any farther forward will risk scraping the tail upon rotation. For our takeoff speed, wing area, mean chord and airplane weight, this position dictates a change in moment coefficient of approximately .5. From Figure G.2, the change in moment coefficient at the stall angle (14.5 degrees, .253 rads) is less than .2. Therefore Figure G.3 shows the necessary Flap effectiveness Parameter of .6. This value translates to a control surface area to tail surface area ratio of .45 and thus an elevator are of 81 $in.^2$.

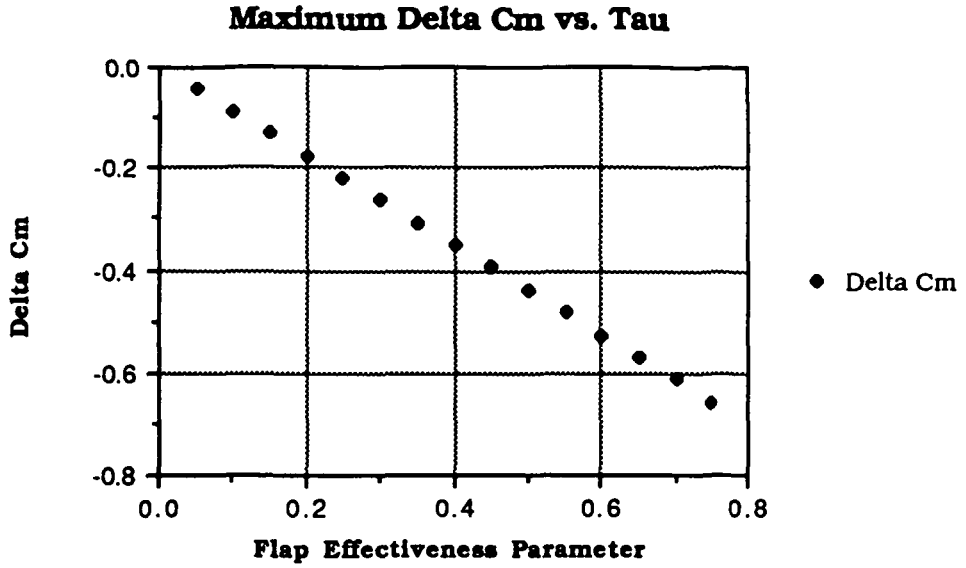

Figure G.3

G.1.5 Summary of Longitudinal Stability And Control Characteristics

Cm,α	-1.51/rad
Cm,o	.203
i_t	1.3 degrees
V_h	.65
AR	4
Airfoil Section	Flat Plate
S_t	180 $in.^2$
Tail Chord	6.7 in.
Tau	.6
S_e	81. $in.^2$
Max. Delta Cm	.52

G.2 LATERAL AND DIRECTIONAL STABILITY AND CONTROL

Directional stability and control will be achieved with an aft vertical tail with a rudder. Lateral stability will be achieved with a high wing with dihedral. As with longitudinal stability, it is crucial for a civil transport aircraft to be very stable. In order to sell "El Toro", the aircraft must be comfortable. In order to fit in the five foot gates, our aircraft has hinged wings. The hinged wings neccessary for the gate requirements make aileron control difficult. Therefore, a powerful rudder along with wing dihedral will effect roll for the "El Toro".

G.2.1 Vertical Tail

As with the horizontal tail, some standard rules of thumb and general trends from previous RPV's gave some starting points which simplified the analysis. An effective aspect ratio of 2.75 and a vertical volume ratio of .255 were used.These values gave the dimensions of the vertical tail on our aircraft.

The expression for the yawing moment coefficient is

$$C_n = V_v \eta_v Cl\alpha_v (\beta + \sigma)$$

Where Beta is the sideslip angle and Sigma is the sidewash angle. Again Eta was assumed to be near 1. The moment coefficient must be zero at zero sideslip angle in order to trim and the slope must have a positive value in order to achieve static stability. The slope of the moment coefficient curve is given by

$$Cn_\beta = V_v \, \eta_v \, Cl\alpha_v \left(1+\frac{d\sigma}{d\beta}\right)$$

Fortunately reference 1 gives

$$\eta\left(1+\frac{d\sigma}{d\beta}\right)=0.724 + 3.06\frac{S_v/S}{1+\cos\Lambda_{c/4w}} + 0.4\frac{Zw}{d} + 0.009\, AR_w$$

so the value of the moment coefficient slope was calculated to be 1.042/rad. This value provides more than enough directional stability. The Yawing Moment curve is shown in figure G.4.

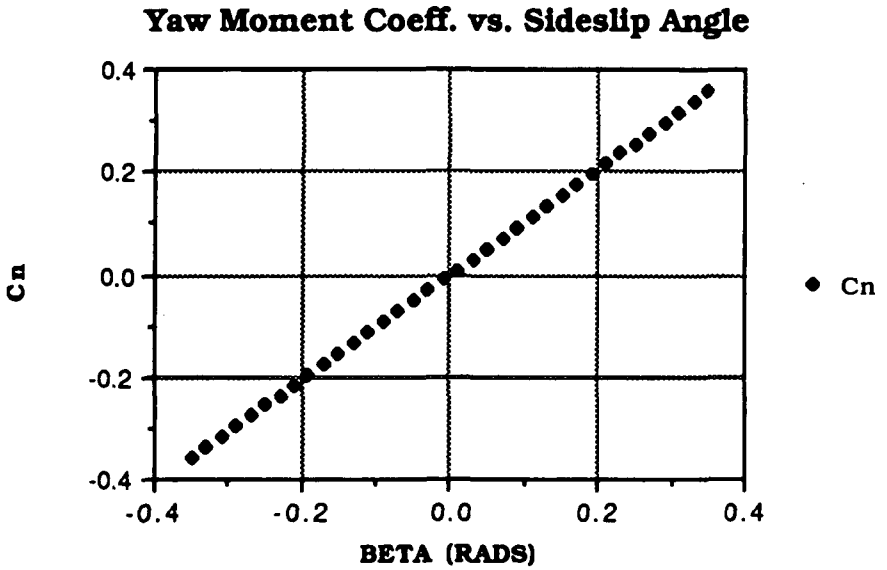

Figure G.4

G.2.2 Directional Control

Directional control of "El Toro" is achieved through the rudder. The rudder deflections change of yawing moment coefficient is given by

$$Cn = -\eta V_V \, Cl,\alpha_V \, \tau \, \delta r$$

Flying indoors should eliminate the need for significant directional control with the exception of the induced sideslip which rolls the aircraft.

G.2.3 Roll Control

Because of the hinged wings, ailerons could not be used to effect roll. Instead, wing dihedral and a powerful rudder were used to roll "El Toro". By inducing a sideslip angle with the rudder, the apparent angle of attack on each wing with dihedral changes by an equal but opposite amount. The resultant change in lift on each wing creates a roll moment. The change in apparent angle of attack is

$$\Delta \alpha = = +/- (\beta \text{ Sin } \Gamma)$$

where Γ is the dihedral angle. We know we can create a moment, but how much dihedral and what rudder size will achieve effective steady state roll?

For civil transport aircraft, a standard rule of thumb states

$$\frac{pb}{2V} = .07$$

where p is the roll rate. This expression gives a necessary roll rate of 30 degrees per second for "El Toro". We also know that we need to bank the plane 30 degrees in order to achieve the 60 foot turning radius at our cruise velocity. Now that we know the roll rate we need to relate it to dihedral and rudder size.

$$p_{ss} = - \frac{L_{\delta r}}{L_p} \Delta \delta r$$

is a relation found in reference 1. This relation uses rudder deflection instead of aileron deflection. We need to come up with an expression

for $L_{\delta r}$, the change in roll moment due to rudder deflection. The first step is relating rudder deflection to sideslip angle. At equilibrium

$$Cn_{\beta}\,\Delta\beta + Cn_{\delta r}\,\Delta\delta r = 0$$

or

$$\frac{\Delta\beta}{\Delta\delta r} = -\frac{Cn_{\delta r}}{Cn_{\beta}}$$

We can also see that change in the moment around the roll axis due to a change in lift in the wings is

$$L=\text{roll moment}= 2\,Q\,S\,Cl\alpha_w\,(\beta\,\Gamma)\,\text{Moment Arm}$$

and

$$\frac{\Delta L}{\Delta\beta} = 2\,Q\,S\,Cl\alpha_w\,(\Gamma)\,\text{Moment Arm}$$

Now

$$\frac{\Delta L}{\Delta\beta}\,\frac{\Delta\beta}{\Delta\delta r} = \frac{\Delta L}{\Delta\delta r} = -\frac{Cn_{\delta r}}{Cn_{\beta}}\,2\,Q\,S\,Cl\alpha,w\,(\Gamma)\,\text{Moment Arm}$$

which along with

$$L_p=C\lambda_p\,\frac{b}{2V}\,Q\,S\,b \quad \text{(this } C_\lambda \text{ is rolling moment coefficient)}$$

and

$$C\lambda_p = -Cl\alpha_w\,/6 \quad \text{(for a zero sweep wing)}$$

and

$$Cn_{\delta r}= -\eta V_V\,Cl\alpha_V\tau$$

gives an expression for steady state roll in terms of equivalent dihedral angle (EDA) and the flap effectiveness parameter. Our aircraft has an equivalent dihedral angle of 13 degrees and a Tau of .75. These values, along with a maximum rudder deflection of 25 degrees, provide "El Toro" with a 30 deg./s roll rate with the rudder fully deflected. Figure G.5 shows some of the trade off analysis done to choose (EDA) and Figure G.6 shows the selection of Tau.

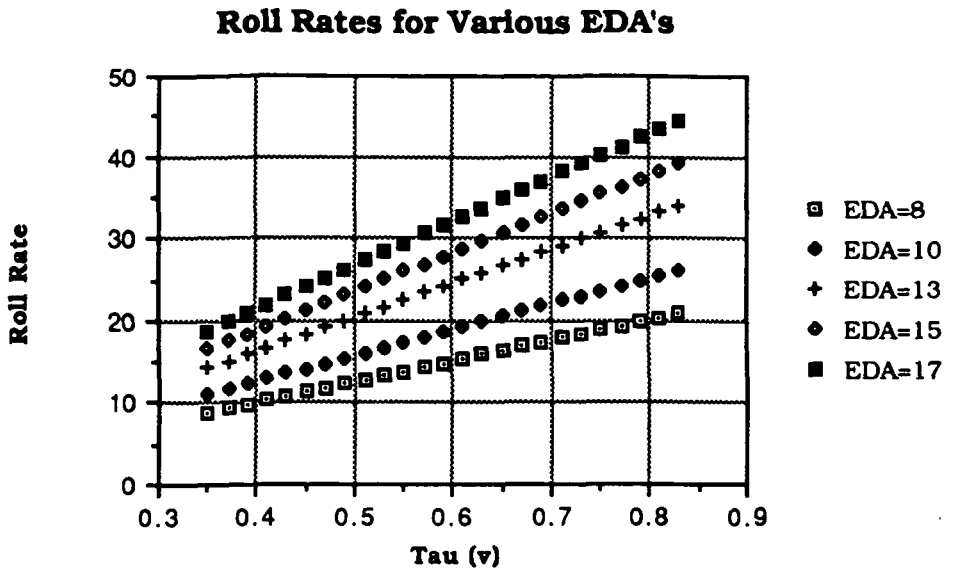

Figure G.5

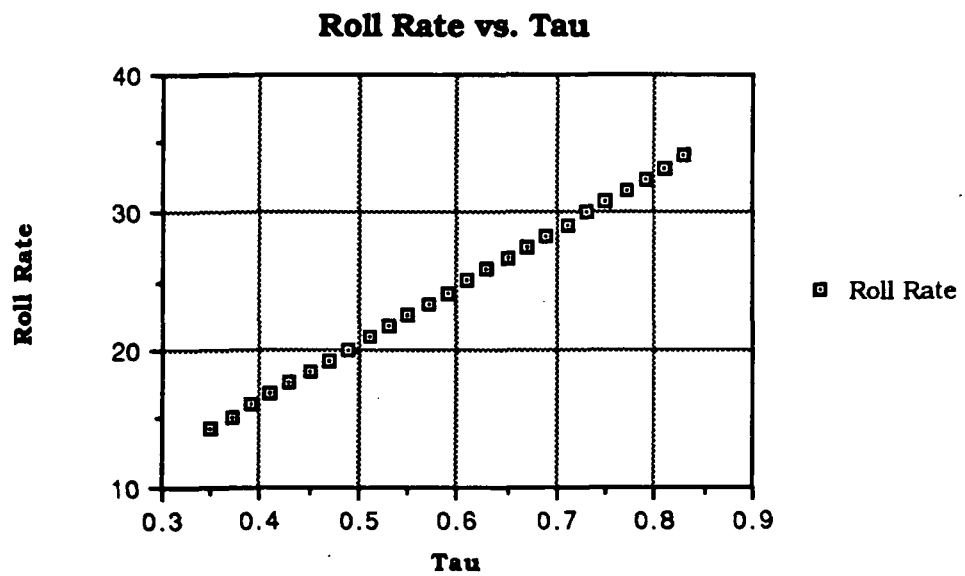

Figure G.6

G.2.4 Equivalent Dihedral Angle

Since we needed to hinge "El Toro's" wing in order to fit it into the required gates, it was convenient to choose a three panel polyhedral design. The panel break is 2 feet in from the wing tips (as far in as possible while folding the wings over) in order to lessen the loss in lift on the outer portion of the wing. An EDA of 13 degrees, with panel break at about half the semi-span, corresponds to a wing deflection of 20 degrees according to reference 2.

G.2.5 Summary of Lateral and Directional Stability Characteristics

Cn_β	1.042/rad
V_v	.255
AR	2.75
Airfoil Section	Flat Plate
S_v	71 in.2
Tail Chord	6.33 in.
Tau_v	.75
S_r	46.2 in.2
EDA	13 deg
Wing Deflection	20 deg
Max Roll Rate	30 deg/s

H. PERFORMANCE ESTIMATION

H.1 TAKE-OFF AND LANDING

The requirements for take-off for an airplane are of utmost importance because the desired take-off performance of an airplane results in the sizing of much of the airplane. From the mission and market studies that were conducted in the beginning of the course it was determined that the airplane should be able to take off within sixty feet. This take-off length requirement sized the motor that was selected. At the time of motor selection, the aerodynamic drag of the aircraft was estimated to be approximately twice the actual value and the overall weight of the aircraft was estimated to range up to six pounds. Because of these two assumptions the Astro 15 motor was selected. For the final configuration of the aircraft, this motor provides more than enough power and a smaller engine would in fact have been sufficient for this airplane. As can be seen from the following graph, the Astro 15 motor has enough power to enable takeoff from <u>any</u> of the airports, thus exceeding the initial design requirements.

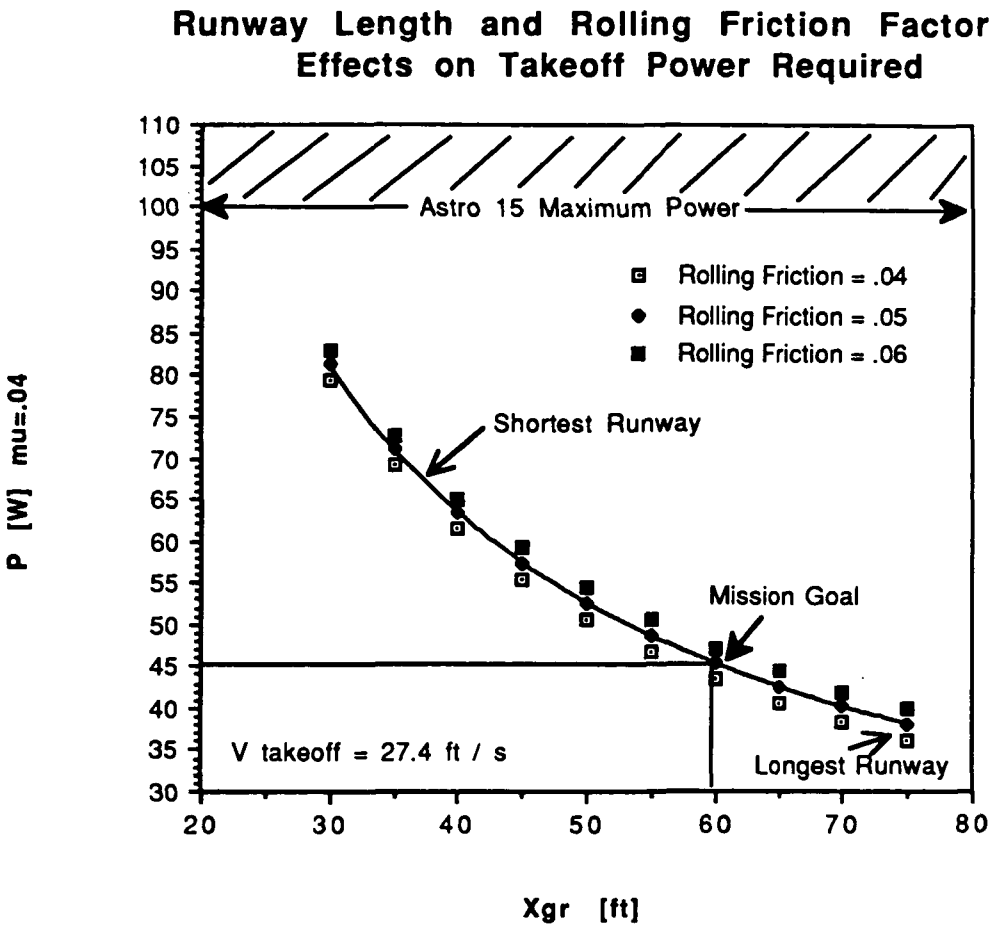

Figure H.1

The success of this aircraft in takeoff entices the designer to overlook the fact that the technology demonstrator will not meet the runway requirements for landing. The technology demonstrator will in fact need in excess of one hundred feet of runway length to land and come to a complete stop. This difficulty will need to be remedied on the actual production aircraft by the design and implementation of a braking system. Due to time limitations, however, this braking system will not be developed for the technology demonstrator.

H.2 RANGE AND ENDURANCE

As previously mentioned, the Astro 15 motor provides more than enough power for this airplane. This overabundance of power is especially true in cruise, allowing the motor to operate at a low power setting, thus increasing range and endurance. The results of long range and increased endurance that this low power setting provides to the performance of El Toro are shown in figure H.2. The original performance objectives for El Toro were a range of 9500 feet and an endurance of 6 minutes. As can be seen from the graph, the current design well out-performs these original goals. The greatest advantage of this increased performance involves operating costs to the airlines. The extended range and endurance allow for numerous flights to be flown before the battery pack needs to be changed. This drastically reduces the operating costs to the airlines allowing them to charge less for a ticket or else to realize a higher profit margin. (For a full discussion on operating costs refer to Section K)

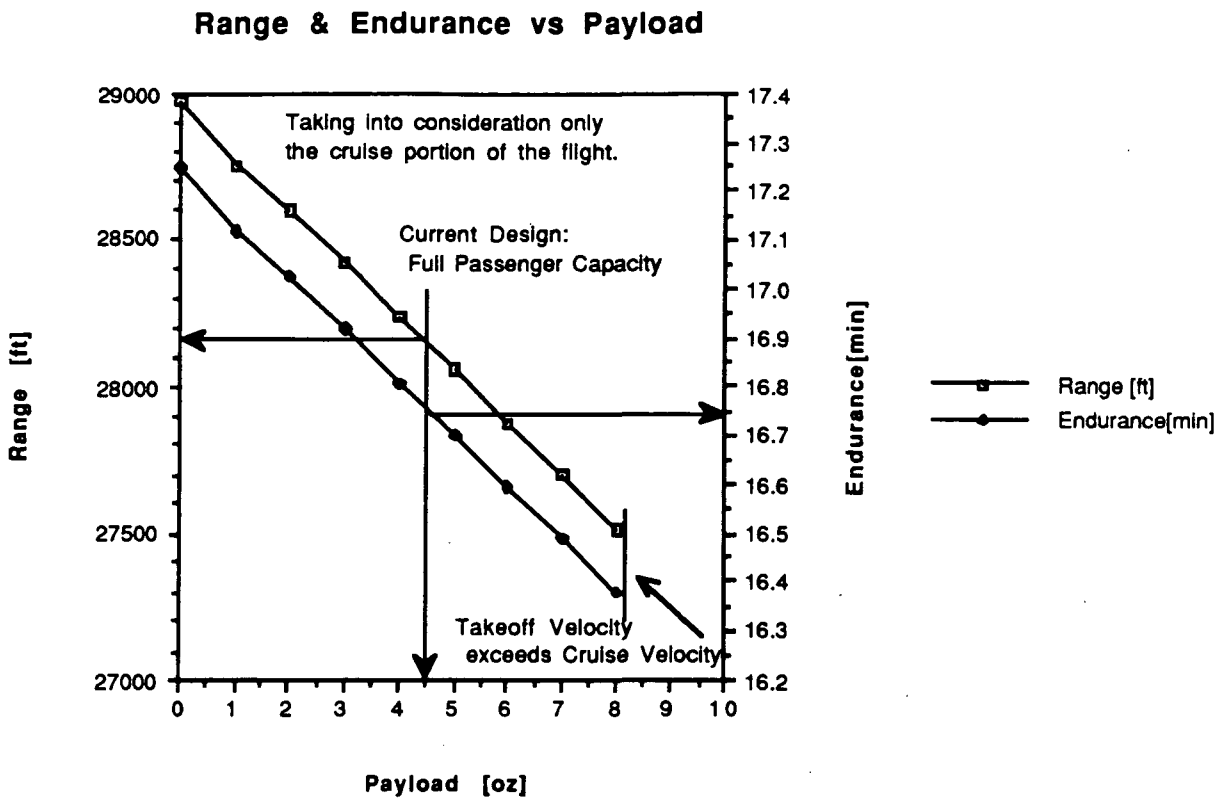

Figure H.2

Figure H.2 shows range and endurance versus payload weight assuming that all of the battery capacity is used during cruise. This neglects the battery power that was used during ground operation, taxi, takeoff and landing. When accounting for the power used during these other phases of the mission, the range and endurance are reduced relative to runway length and time on the ground. For the current airplane with a 1200 mah battery pack the range and endurance are approximately 25000 feet and 16.3 min respectively.

H.3 CLIMBING AND GLIDING PERFORMANCE

Based on a data base of previous RPV aircraft, a desired rate of climb of 6 ft/s was chosen for this aircraft. Once again, because of the high excess power provided by the Astro 15 motor, this goal rate of climb is easily met by the aircraft. The maximum rate of climb for the current aircraft is 14.5 ft / s. Thus, the goal rate of climb can be met at a lower power setting, allowing for a savings in fuel used during climb. The relatively large maximum rate of climb of this aircraft could provide some added safety benefits as it allows the airplane to overcome possible wind gust problems during take-off and landing. Further research will need to be conducted to determine exactly how much of a benefit this provides in overcoming the wind gust problems.

The glide performance of an aircraft is especially important when that aircraft has only one engine and is a passenger aircraft. If that one engine should fail the pilot can not simply eject, but must have enough time to be able to radio for help, find a clearing and land the aircraft. This airplane configuration provides a minimum glide angle of approximately 3.5°. This provides the pilot with about 300 feet and 10 seconds until the aircraft touches down. Further studies should be conducted to find out if this is an adequate range and time for a successful non-powered landing.

H.4 SUMMARY OF PERFORMANCE DATA

Velocity	
Cruise:	**28.0 ft / s**
Stall:	**22.8 ft / s**
Maximum:	**76.5 ft / s**
Range	
@ Cruise:	**25000 ft**
@ Rmax:	**33000 ft**
@ Emax:	**30000 ft**
Endurance	
@ Cruise:	**16.3 min**
@ Emax:	**16.6 min**
@ Rmax:	**15.8 min**
Takeoff Distance	
Desired:	**60.0 ft**
Minimum:	**23.8 ft**
Landing Distance	
Desired:	**60.0 ft**
Minimum:	**100 ft**
Rate of Climb	
Desired:	**6 ft / s**
Maximum:	**14.5 ft / s**
Glide Angle	
Minimum:	**- 3.5°**

J. STRUCTURAL DESIGN

J.1 INTRODUCTION

In order to complete the design of the aircraft structures several tasks needed to be performed. First, the estimation of the ground and flight loading needed to be investigated. From these load analyses the overall load factor the aircraft will experience was calculated. Next, the structure needed to be broken down into several basic components. Finally, the design of each substructure needed to be completed.

The substructure design process included several steps. First, the particular loading that the structure must endure was examined. Next, the material needed to withstand these stresses are chosen. Finally, the detailed sizing of the frames were conducted.

J.2 LOADING

There are two major areas where the loading of the aircraft was investigated. First, the loads experienced by the structure during the period it was on the ground was calculated. When the aircraft is on the ground, it will experience three distinct types of load. See Figure J.1 for loading scheme. First, three 1.7 lb concentrated point loads are being applied by the landing gear at the location where they are attached to the fuselage. There are also two distributed loads actting along the x and y axis of the aircraft. Along the y axis the structure is

being stressed by the weight of the wing. The bending moment at the root chord was calculated with this equation

$$M=ww\ (span)/2 \qquad (J\text{-}1)$$

where ww was the weight of the wing. The bending moment equalled 1.57 ft lb. Finally, along the x axis the structure is being stressed by the force of the landing gear, the weight of the fuselage, and weight of other aircraft components. Figure J.2 and Figure J.3 were shear and moment diagram, respectively, calculated from these loads.

Figure J.1: Ground Loads

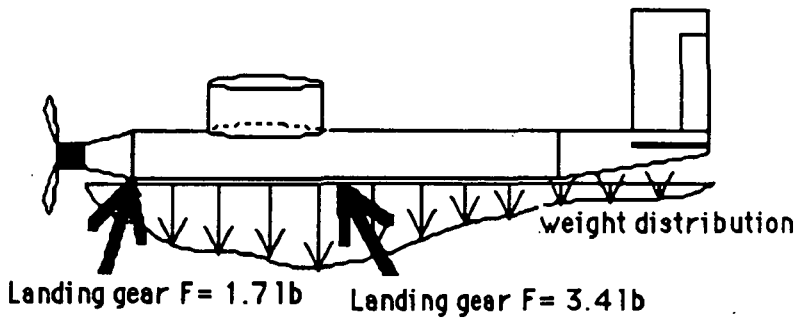

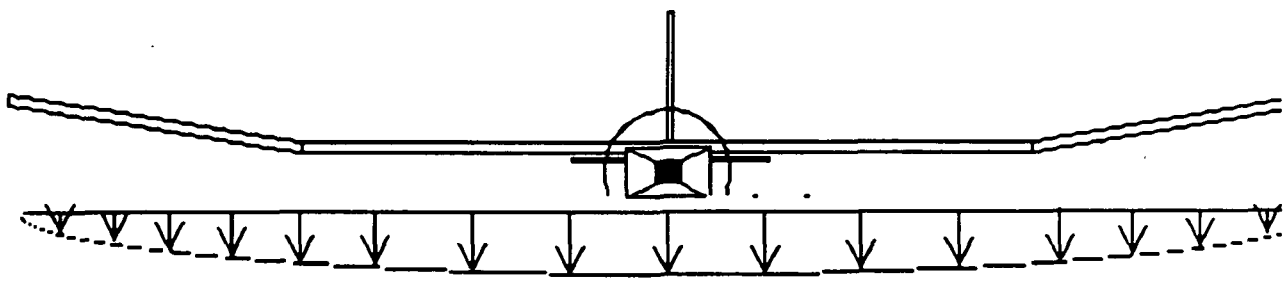

weight distribution

Because the aircraft will spend the duration of its time in flight and the aircraft will experience the most stresses during this period, the loading during flight was the greatest consideration of the structural design. There are three basic loads being applied to the aircraft during flight. First, there is the weight of each component acting in the negative z direction. Next, there is the distributed lift provided by the wing airfoil. Finally there are the forces and subsequent moments caused by the deflection of the control surfaces. Further details on these forces will be given in the corresponding substructure design section.

Figure J.2: Fuselage Shear Diagram-ground load

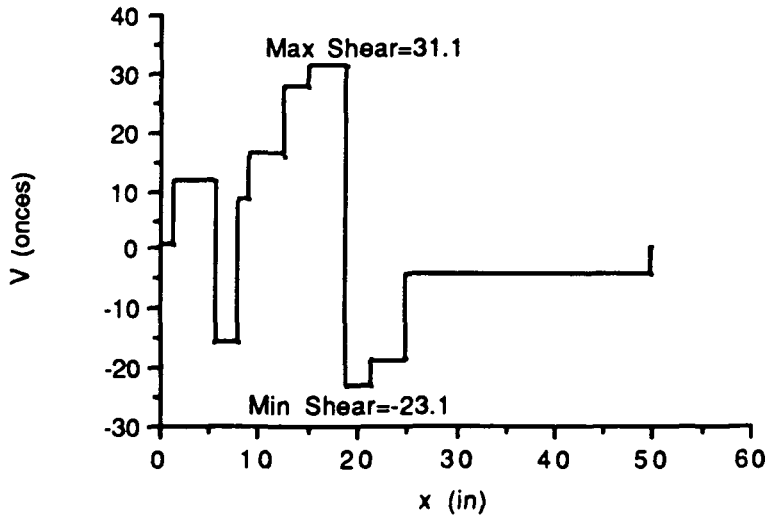

Figure J.3: Fuselage Moment Diagram-ground load

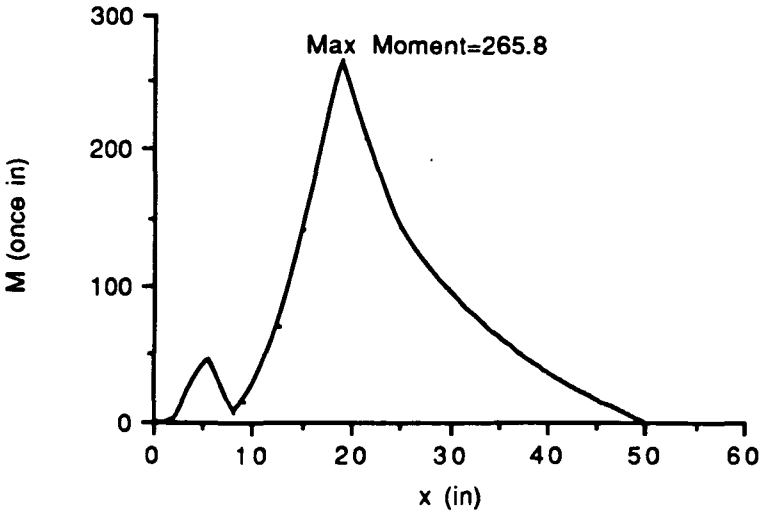

J.3 LOAD FACTOR

The next integral part of designing an aircraft structure is to calculate the expected load factor the plane will experience during its flight. There are three major areas of investigation: taking-off, turning and landing. For taking off, the load factor (n) was defined as follows

$$n = 1 + a/g \qquad \text{(J-2)}$$

where g was the acceleration due to gravity and a was the vertical acceleration of the plane at takeoff. Assuming that the aircraft will takeoff at 55 ft traveling 27.4 ft/s, the aircraft has approximately 3.5 seconds before it must turn. During this time the plane must also reach an altitude of 15 ft; therefore requiring a 4.3 ft/s rate of ascent. Assuming that the propulsion system will provide this rate of climb within 1 second, the acceleration needed to increase the vertical speed from 0 ft/s to 4.3 ft/s was calculated to be 4.3 ft^2/s with the corresponding load factor of 1.13.

During a turn there were several factors which influenced the load factor: velocity, radius, and weight. The load factor was calculated with the following equation

$$n = \text{lift/weight} \qquad \text{(J-3)}$$

The required lift was calculated with the following equation

$$\text{lift} = (lz^2 + ly^2)^{.5} \qquad \text{(J-4)}$$

where lz and ly are the lift in the z and y direction respectively. Assuming that the plane must maintain its altitude during the turn, lz must equal the weight, 5 lb. Ly was calculated using the following equation

$$ly = \text{mass} (\text{velocity}^2) / \text{radius} \qquad \text{(J-5)}$$

where the radius was set at 60 ft and the velocity equalled 28 ft/s. From this the load factor was calculated to be 1.08.

Finally the load factor at landing was calculated using equation J-1 where a was the vertical deceleration at touchdown. Assuming the plane begins to descend half way through the final turn traveling at the cruise velocity, the aircraft has 3.4 seconds to drop 15 ft. This corresponds to 4.5 ft/s rate of descent and a 1.14 load factor. Using a factor of safety of 1.2 the limit load factor was calculated to be 1.36. See Figure J.4 for the V-n diagram.

Figure J.4: V-n Diagram

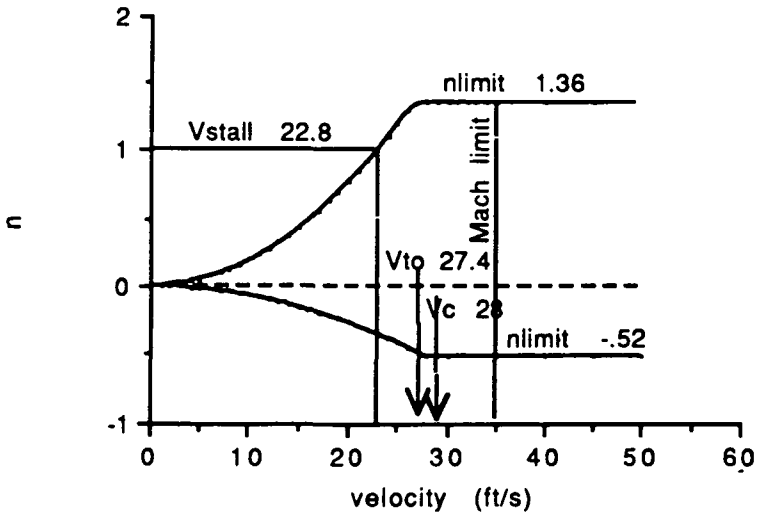

J.4 STRUCTURAL COMPONENTS

To meet the requirement of fitting in a 2'x3'x5' storage container and to make construction easier, the aircraft structure was divided into two components, wing and fuselage, with several substructures. The wing has three substructures: center section and two wing tips. On the other hand the fuselage has six substructures: engine mount, 2 main fuselage sections, empennage, vertical tail and horizontal tail.

J.4.1 Wing

Before designing the wing, the loadings that the wing will experience were investigated. The wing will be stressed by two distributed forces, lift along the span and weight of the wing section. Assuming the required lift would be 5 lb times the load factor, 1.36, and that the wing structure will weigh .75 lb, a shear and moment diagram was completed. See Figure J-5 and J-6 for the shear and moment diagram respectively.

Figure J.5: Shear Diagram

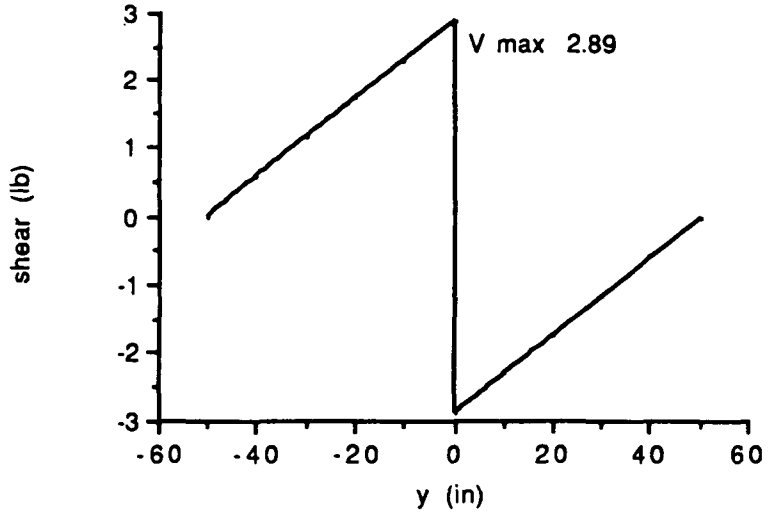

Figure J.6: Moment Diagram

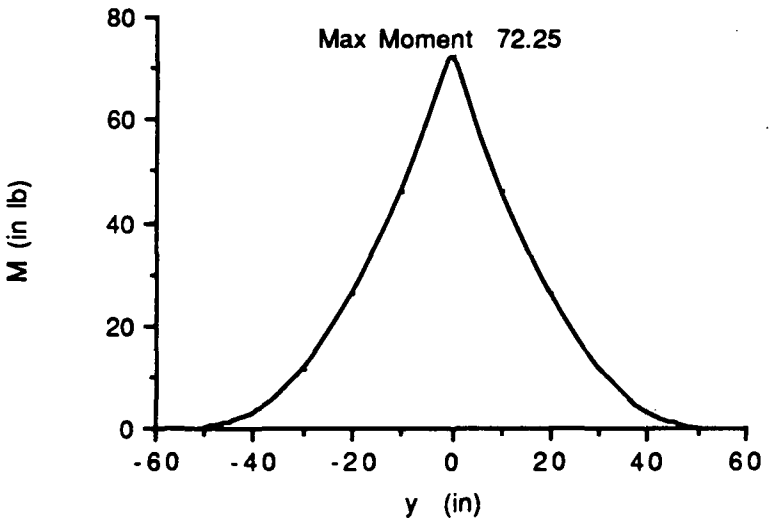

The figures clearly show that the wing section at the root chord will be exposed to the greatest stress; therefore logically, the wing design must withstand 6.02 ft lb bending moment. A structure with three spars, one located at the airfoil maximum thickness (30% chord) and two located at the two ends seemed sufficient to withstand

the stresses. Because they were located close to the centroid, the leading and trailing edge spars will not carry much of the load; however they helped to maintain the airfoil shape. With this function in mind the shape and dimensions of the spars were set. The leading edge spar will be circular with a radius of .125 in. The trailing edge spar will be triangular with a base of 1 in and a height of .25 in. Both of these spars will be constructed out of balsa wood to reduce weight.

The shape of the main spar underwent several evolutions. First the spar was shaped as a solid beam made of one material. The stress due to bending was calculated with the following equation

$$\text{stress} = M(y)/I \qquad \text{(J-6)}$$

where M is the bending moment, I is the moment of inertia and y is the distance from the centroid. Next, the material for the beam was chosen. Using a simple TKSolver program which varied the beam thickness while calculating the maximum stress and weight, four materials were compared to see which would be the best material for the beam. Figure J-7 is a plot of the weight verses stress for the four materials with the end point at the stress limit for that material. From this graph spruce was chosen as the material to be used for the main spar.

Figure J.7 : Material Selection

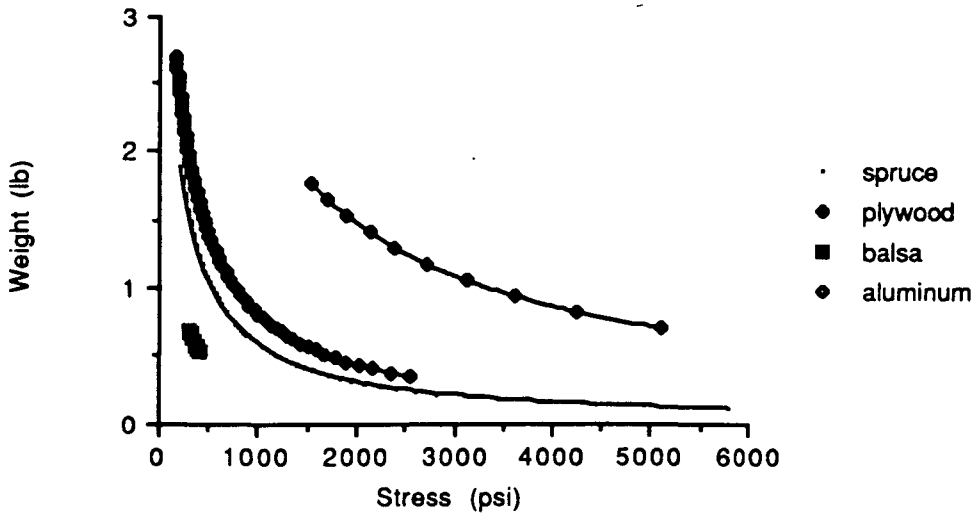

Next the shape of the spar was investigated to provide the best support with the least weight. Three shapes were considered: solid beam, two square beams located at the two extremities and an I beam (see Figure J.8). The solid beam was disregarded because it weighs the most of the three while providing negligible strength advantages. Although the two squares were able to withstand the stress due to bending, they were not stiff enough to prevent wing twist. Therefore out of the three, only the I beam was able to provide the necessary strength while still maintaining the required low weight.

Figure J.8: Spar Concepts

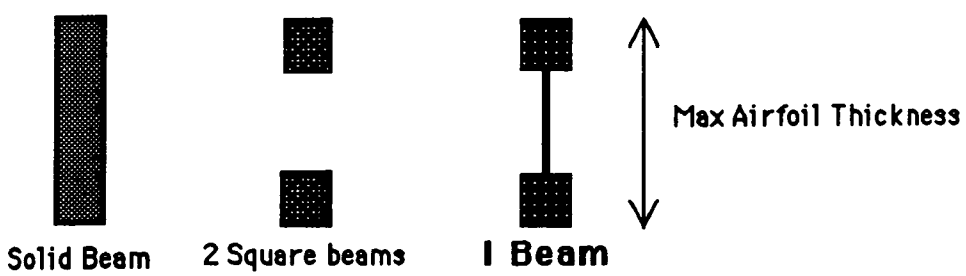

In the final analysis of the I beam it was discovered that the web was exposed to shearing stresses close to the spruce shear stress limit, 750 psi. To correct this situation, birch plywood was used for the I beam web because the plywood's shear stress limit was 7500 psi; however this extra strength came with an additional weight penalty.

To provided sufficient airfoil shape integrity, the ribs were spaced 5 inches apart with an additional three ribs placed at the two hinge locations and the root chord. See Figure J.9 for the final wing design.

Figure J.9: Wing Design

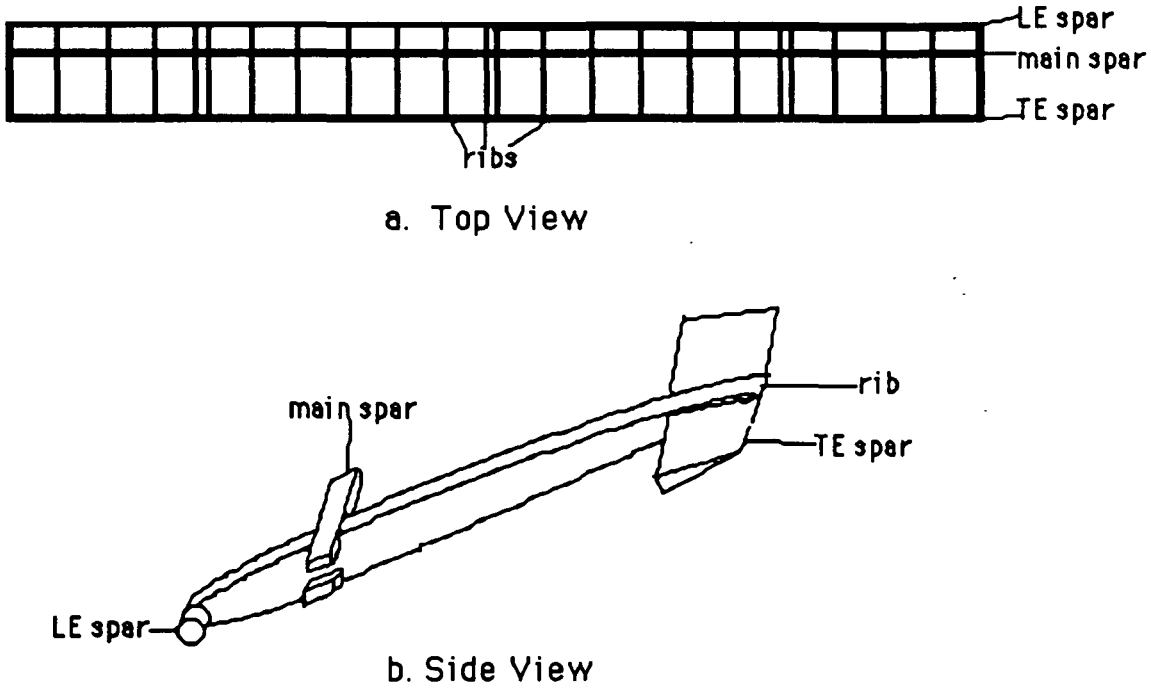

J.4.2 Wing Hinge Design

One of the most critical areas in our plane's structural configuration is the hinge design of the wing. The feasibility of this technology must be demonstrated in order to justify our plane design. Without folding wings, our plane would not meet the gate requirements of Aeroworld. One of the primary purposes of the technology demonstrator will be to show that a working folding wing can be constructed.

The wing will fold at 2.5 feet out along the span from the centerline, where the dihedral begins; thus, 20% of the entire span will be folded at each end. The hinge design will have to be able to sustain the internal forces and moments created by the lift produced by the folded portion when in flight. For the technology demonstrator, the wings will be folded manually but on a full-scale plane some means would have to be incorporated, either on the plane or ground. A hydraulic system on the plane would increase the wing weight, while using a ground-based system would likely increase the ground time.

The hinge will consist of a tab on the dihedralled portion of the wing which will insert into the main part of the span along the main spar. Two pins will attach the tab to a slot in the main spar. In addition, the leading and trailing edge spars will be clipped together to resist twist and bending. The clips and the lower pin will be removed on the ground so that the wing can be rotated up about the remaining pin. The two closely placed ribs will give additional support. The tab and pins of the hinge will be constructed of hardwood in order to help prevent failure. Additionally, on the actual

plane an elastic skin/cowling would be used to reduce the drag created by the exposed portion of the hinge.

J.4.3 Fuselage Design

The fuselage can be broken down into several substructures. The first substructure is the engine mount. To provide enough room for the engine 5 in. of the fuselage was alloted. This section was tapered to streamline the fuselage and reduce the drag. Two materials are used to construct this section. First, all the beams are made out of spruce because spruce can provide adequate strength to reduce the vibration of the engine. However the firewalls were constructed out of plywood to withstand the shear from the nails used to attach the engine. See Figure J.10 for the final design.

Figure J.10: Engine Mount Design

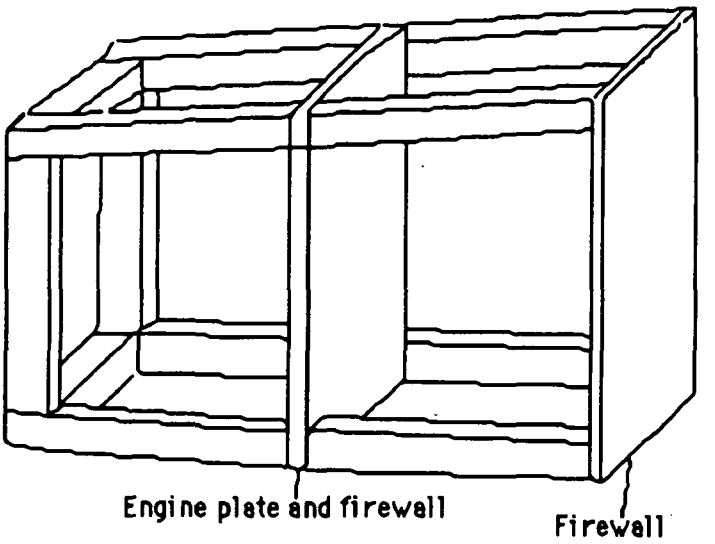

To compliment the tapered front of the fuselage, the fuselage also has a tapering tail end. This section is 14 in. long and experiences some considerable loading. First the lift, .4 lb, provided by the horizontal tail produces a moment of .5 ft lb in the y direction at the junction of this section to the fuselage. Also the side force produced by the vertical tail equals .35 lb and causes .175 ft lb of moment in the z direction. The stresses will be carried by four beams which run the length of this section. Using TKSolver the dimensions of the beam was calculated to be .25" x .2". These beams will be aided by .2"x .2" vertical and horizontal posts, which provided additional strength and maintained the airfoil shape. Finally to provide additional support against bending .125" x .25" diagonal beams placed along the vertical and horizontal face of the fuselage. See Figure J.11 for the final design.

Figure J.11: Tapered Fuselage Design

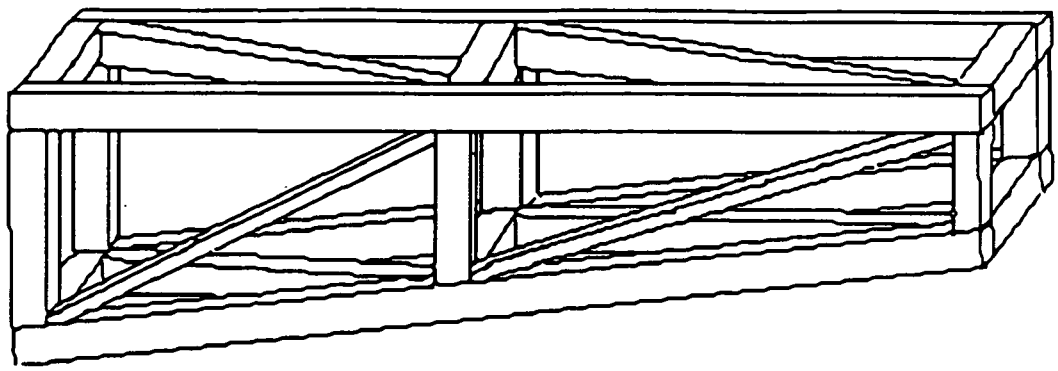

At the end of the tapered fuselage there is another minor substructure of the fuselage: the horizontal and vertical tails. Because these control surfaces will only be flat plates, the structural design is relatively simple. The perimeter of the tail will be lined with .2'x.125' beams. For the internal structure there are four crisscrossing diagonals of the same dimensions. This pattern is maintained for the rudder and elevator also. See Figure J.12 for the final design of the control surfaces.

Figure J.12: Basic design for Control Surfaces

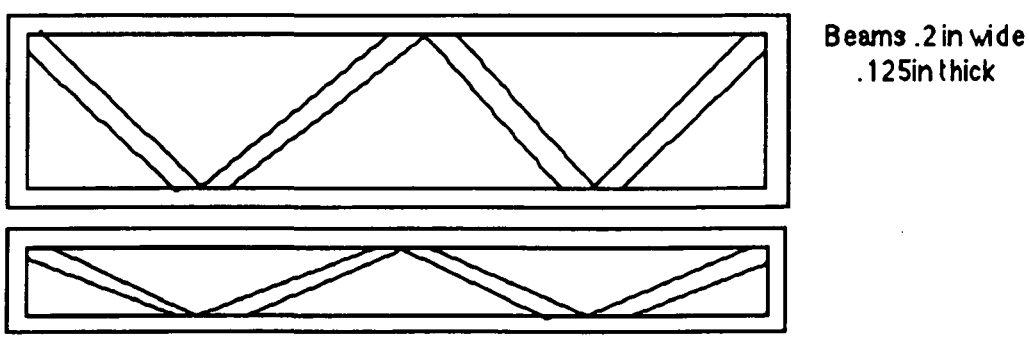

Finally the last two fuselage substructures are the fuselage sections under the wing and the section beyond this section. First, the forces

acting on the fuselage were identified. These forces included the wing lift and the weight of the different aircraft systems. Using these loadings shear and moment diagrams were created. See Figure J.13 and J.14 for the shear and moment diagrams.

Figure J.13: Fuselage Shear Diagram

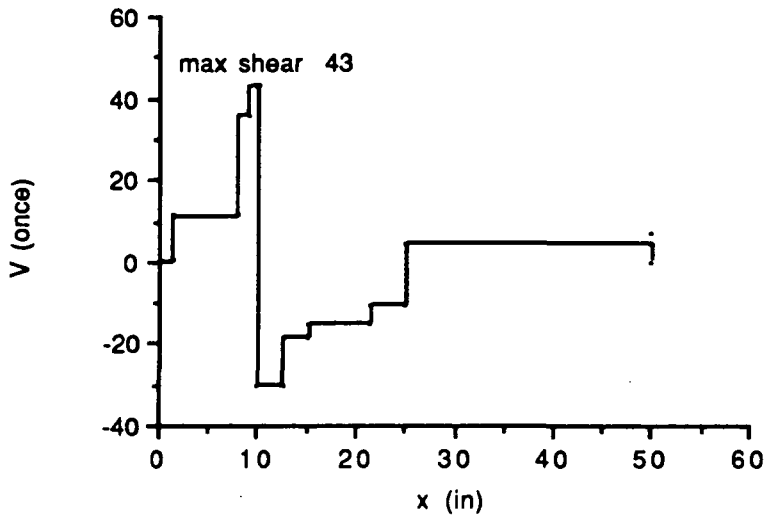

Figure J.14: Fuselage Moment Diagram

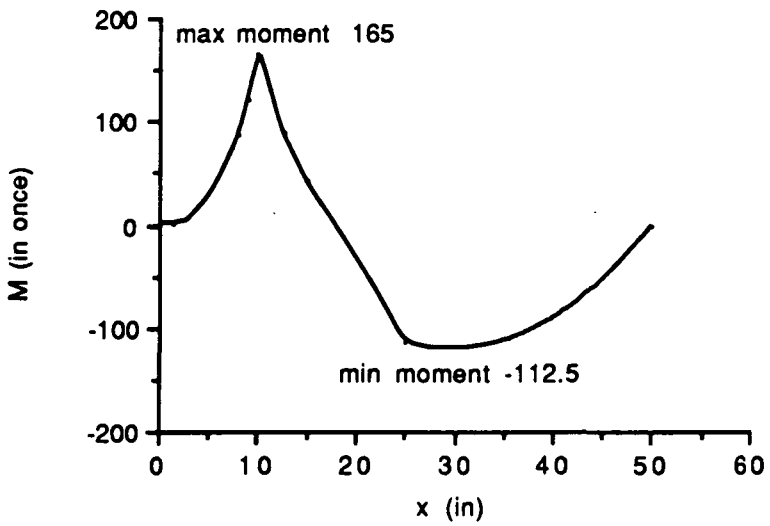

The first substructure has a length of 14 in. and contains two levels. The top level is designed to hold the battery, servos and receivers,

while the passengers sit on the bottom section. Not only will this structure have to support the two platforms but it must also support the landing gear placements. Because of this the entire structure is constructed out of spruce material. Like before, four beams running the length of the section will carry the majority of the load. Knowing that the max shear is 43 onces and max moment is 265.8 inch once (from ground load bending), the beam sizes are calculated to be .25"x.2" by using TKSolver iterations. In addition to the four longitudinal beams, there are 4 sets of two .2"x.2" vertical posts added to give further support. Also .2" x .2" transverse beams were used to give the fuselage the rectangular shape. Two transverse beams on the top was omitted to provide easy acess to the batteries. Because the .125 in plywood platform will be attached to the posts, there is no need for diagonal buttresses. See Figure J.15.

Figure J.15: Battery Platform and Fuselage Design

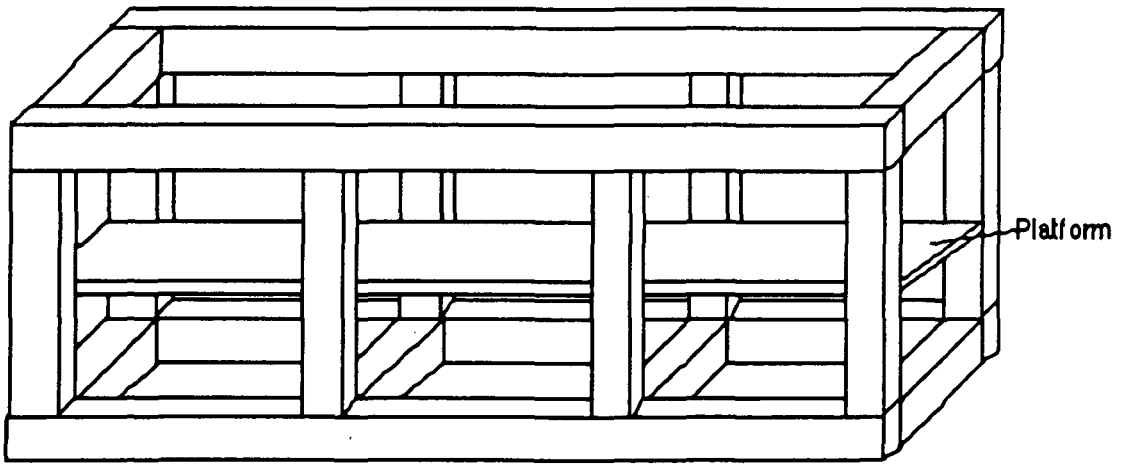

Finally the last section, the 17 inch main passenger section, needs to be designed. Using the moment and shear diagrams, the max shear

is calculated to be 15 ounces and the max bending moment is 112.5 in once. Because this section does not experience as much loading as the other fuselage section, the material used for the beams is balsa. Again four longitudinal beams are used to carry the majority of the load. Using the same TKSolver program the size of these beams is calculated, but to make the structure more continuous the recommended size is increased to equal .25"x.2". In addition to the four beams, five sets of four posts are used to maintain fuselage shape. Finally to add additional support, twelve diagonal .125"x.2" beams are attached to both sides of the fuselage; however none are needed on the top or bottom because the main bending was around the y axis not the x axis. See Figure J.16 for the final design.

Figure J.16: Main Fuselage Design

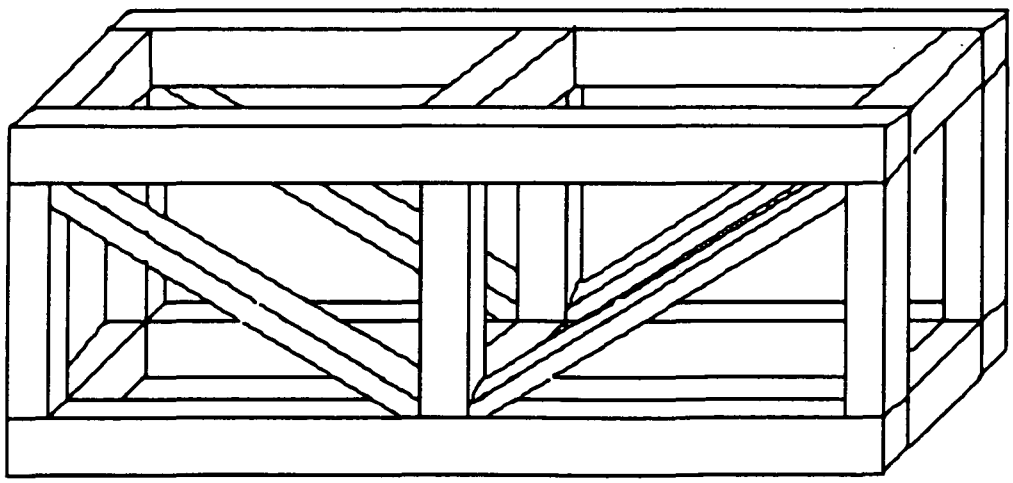

K. DERIVATIVE AIRCRAFT

One concern when designing an aircraft is the possibility of future derivative aircraft. The original design objective for this project was a commercial passenger transport to be sold to airline companies in Aeroworld. The aircraft currently proposed carries 51 passengers with luggage, and includes area in the tail of the fuselage for galleys and restrooms. Derivative aircraft with a fuselage of different length could easily be constructed. The power supply (a major contributor to weight) and control system will be placed to maintain the center-of-gravity near the quarter-chord of the wing. There is also allowance made to move the power supply forward or aft from its current position to control the center-of-gravity movement. This enables derivative aircraft to be built with a longer or shorter fuselage to meet future airline needs and still maintain the center-of-gravity near the quarter-chord of the wing. A longer fuselage would cause the center-of-gravity to move aft and a shorter fuselage would cause the center-of-gravity to move forward. The power supply could be moved forward and aft, respectively, to counter this center-of-gravity shift.

The proposed aircraft also has a relatively large, open fuselage. Passenger seating, luggage compartments, galleys, etc could be removed to create a spacious, empty fuselage. This makes conversion from civil passenger transport to cargo transport easy and cost efficient. A cargo transport could actually be constructed at lower cost because seating, galleys, and luggage structures would be left out entirely. The proposed aircraft could also be constructed to meet

military transport needs. Cargo or passengers needs or a combination of both could be met in derivative aircraft.

A final derivation of the proposed aircraft involves the engine. The current engine possesses much greater power and range than is necessary. This does have benefits as discussed earlier, but a smaller engine could be used if desired.

L. TECHNOLOGY DEMONSTRATOR

The final part of the design of "El Toro" was the validation of the technology in the form of a prototype aircraft. The prototype will demonstrate the airworthiness of the aircraft and provide actual performance data to compare to design data. The significant aspects of the technology demonstrator at this point are the final configuration, the costs, the weight and construction problems.

L.1 CONFIGURATION

The final configuration of our technology demonstrator matches very well with the design submitted. The only differences lie in the areas in which our initial design was ambiguous. The chief areas of interest being the detailed structural design and the hinge in the wing. The initial design of the structure did not take into account the stregnth of the mylar coating. The mylar adds tremendous stregnth and durability to the design. So much stregnth was added that lighter weight components could have replaced much of the spruce and other large portions of our structure.

The initial hinge design had a 1/4 inch gap between the wing sections. Due to lack of construction experience and proper tools, the smallest hinge feasible was 1/2 to one inch. The dimensions of the technology demonstrator, however, were identical to the design.

L.2 COST

(All listed costs are in 'real world' money. Aeroworld totals are at the bottom)

Propulsion

Astro 15 electric motor	$105
Speed Controller	$70
batterries	$26
Zinger 10-6	$3
Propulsion Subtotal	$204

Avionics

Radio Receiver/Transmitter	$116
Servos	$66
Control Rods	$5
Avionics Subtotal	$187

Structures

Mylar	$20
Balsa/Spruce	$40
Landing Gear	$15
Tail Hinges	$2
Glue	$10
Structures Subtotal	$87

Material Subtotal	$478
x $400 (Aeroworld money)	**$ 191,200**

Labor

125 man hours x $100 (A.W. money) **$12,500**

Total Prototype Cost (A.W. money) **$203,700**

These costs represent the prototype development costs. In future production of aircraft, Betasystems is confident that man hours and material waste will reduce the cost dramatically.

L.3 WEIGHT

Main Fuselage	14.5	15.0
Wing	12.0	14.0
Propulsion	11.0	9.05
Batteries	24.0	21.3
Landing Gear	3.5	7.1
Avionics	7.5	7.5
Empennage	2.5	3.0
Total	80.0	81.35

The center of gravity estimation was very close to the actual value with the initial battery location . The wide range of possible battery positions allowed for fine tuning of the center of gravity location to 30% of the mean chord.

L.4 CONSTRUCTION

Spruce made up the forward half of the main fuselage frame as well as the nose. Balsa was used for the tapered part of the fuselage, the rear of the passenger section, as well as the horizontal and vertical tail. A plywood plank was put in the forward portion of the fuselage to hold the batteries, receiver, speed controller and servos. Two sections of plywood also made up the firewalls. The wing used balsa airfoil sections, wingtips, leading and trailing edges. Spruce was used for the main spars as well as the hinges.

The hinges employed simple spruce extensions from the main spar cut at the appropriate angles. Two extensions from one wing section slid in next to the two extensions from the other section. Two screws were then drilled through the four surfaces.

The rear landing gear was screwed into a plywood section which glued onto the bottom of the fuselage. The mount for the front gear was screwed into the forward firewall. The landing gear was not attached to the fuselage until after the fuselage was complete. This lead to difficulty attaching the front gear to the rear firewall. Drilling the gear mount into the firewall before attaching the firewall to the fuselage would have been prudent.

Inexperience with the mylar coating led to a certain amount of sag between ribs in the wing. This sag led to a wing without a constant airfoil section. This inconsistency could lead to less lift than predicted in the initial analysis.

The construction of the technology demonstrator was made more difficult due total lack of experience and a lack of direction or

helpful hints about technique from 'upper level management'. Simple hints, like the fact that mylar does not bond to glued surfaces well, would have produced a more aesthetically pleasing, as well as a more airworthy, technology demonstrator. Overall the construcion of the aircraft went smoothly. In the initial structural design process, a main criteria was ease of construction. This criteria was chosen with knowledge of the group's construction inexperience and an effort to minimize construction costs by lowering labor hours. In retrospect, this criteria served the group well by eliminating many construction complications.

Appendix A

Request for Proposal

A. REQUEST FOR PROPOSAL

A.1 COMMERCIAL AIR TRANSPORTATION SYSTEM DESIGN

Commercial transports operate on a wide variety of missions ranging from short twenty minute commuter hops to extended fourteen hour flights which travel across oceans and continents. In order to satisfy this wide range of mission requirements "families" of aircraft have been developed. Each basic airplane in the family was initially designed for a specific application but from that basic aircraft numerous derivative aircraft are often developed. The design of the basic aircraft must be sensitive to the fact that derivative aircraft can be developed.

Though they may differ in size and performance, all commercial designs must also possess one common denominator; they must be able to generate a profit which requires compromises between technology and economics. The objective of this project is to gain some insight into the problems and trade-offs involved in the design of a commercial transport system. This project simulates numerous aspects of the overall systems design process so that exposure to many of the conflicting requirements in a systems design are encountered. In order to do so in the limited time allowed for this single project a "hypothetical world" has been developed and information on geography, demographics, and economic factors have been provided. This project is formulated in such a fashion that each group is asked to design a basic aircraft configuration and derivative aircraft which will have the greatest impact on a particular market. The project does not

allow for a performance of s systems design study but does provide an opportunity to identify those factors which have the most significant influence on the system design and design process. Formulating the project in this manner allows for the opportunity to fabricate a prototype of the designed aircraft and develop the experience of transitioning ideas to "hardware" and then validate the hardware with prototype flight testing.

A.2 PROBLEM STATEMENT

The project goal is to design a commercial transport which will provide the greatest potential return on investment in a new airplane market. Maximizing the profit that each airplane design will make for the customer, the airline, is the design goal. Each group may choose to design the plane for any market in the fictitious world from which they believe the airline will be able to realize the most profit. This is done by careful consideration and balancing of the variables such as the number of "passengers" carried, range/payload, fuel efficiency, production costs, and maintenance and operation costs. Appropriate data for each is included later in the project description.

The "world" market in which the airlines operate is shown in Figure 1. Table 1 gives the number of people who wish to travel between each possible pair of cities each day. (Note: that Table 1 is symmetric about its diagonal.) Table 2 gives other useful information regarding each city: details on location, runway length (Length=factor x 75 ft) and number of gates available to each airline and their size. The up-start airline may operate in any number of markets provided

that they use only one airplane design and its derivatives (the company does not have the engineering manpower to develop two different designs for them). Consideration of derivative aircraft is a possible cost-effective way of expanding its market.

A.3 REQUIREMENTS

1. Develop a proposal for an aircraft and any appropriate derivative aircraft which will maximize the return on investment gained by the airline through careful consideration and balance of the number of passengers carried, the distance traveled, the fuel burned, and the production cost of each plane. The greatest measure of merit is associated with obtaining the highest possible return on investment for the airline. Each group is expected to determine the "ticket costs" for all markets in which they intend to compete. The proposal should not only detail the design of the aircraft but must identify the most critical technical and economic factors associated with the design.

2. Develop a flying prototype for the system designed above. The prototype must be capable of demonstrating the flight worthiness of the basic vehicle and flight control system and be capable of verifying the feasibility and profitability of the proposed airplane. The prototype is required to fly a closed figure "8" course within a highly constrained envelope. A basic test program for the prototype must be developed and demonstrated with flight tests.

A.4 BASIC INFORMATION FOR "AEROWORLD"

The following information is used to define special technical and economic factors for this project. Some are specific information, others are ranges which are projected to exist during the development of this airplane. (Note: real time is referred to as RWT, Aeroworld time as AWT.)

1. Passengers: Standard Ping-Pong balls - Remember these are "passengers" not cargo, therefore items like access, comfort, safety, etc. are important.
2. Range: distance traveled in feet
3. Fuel: battery charge in milli-amp hours (RWT)
4. Production cost = $400 per dollar spent on the prototype + $100 per prototype construction man-hour (RWT)
5. Maintenance (timed battery exchange) = $500 per man-minute (RWT)
6. Fuel costs = $60-$120 per milli-amp hour RWT
7. Regulations will not allow the plane to produce excessive "noise" from sonic booms; consider the speed of sound in this "world" to be 35 ft/s.
8. the typical runway length at the city airports is 75 ft, this length is scaled by a runway factor in certain cities.
9. Time scale is 1 minute AWT = 30 RWT minutes
10. The world has uniform air density to an altitude of 25 feet and then is a vacuum.
11. Propulsion systems: The design, and derivatives, should use one or a number of electric propulsion systems from a family of motors provided by the instructor.

12. Handling qualities - To be able to perform a sustained, level 60 ft. radius turn.

13. Loiter capabilities - The aircraft must be able to fly to the closest alternate airport and maintain a loiter for one minute AWT.

14. There are two existing modes of transportation in Aeroworld which offer competition to the airline market:

An average train fare costs $6.25 per 50 ft + $50 flat rate

An average ship fare costs $8.00 per 50 ft + $65 flat rate

A.5 SPECIAL CONSIDERATIONS FOR THE TECHNOLOGY DEMONSTRATOR

The prototype system will be an RPV and shall satisfy the following:

1. All basic operation will be line-of-sight with a fixed ground based pilot, although automatic control or other systems can be considered.

2. The aircraft must be able to take-off from the ground and land on the ground under its own power.

3. The prototype flight tests will be conducted within a restricted range on a figure "8" course with a spacing of 150 ft between the two pylons which define the course. The flight tests for the Technology Demonstrator will be conducted in the Loftus Center (Figure 2) on a closed course. The altitude must not exceed 25 ft at any point on the course.

4. The complete aircraft must be able to be disassembled for transportation and storage and fit within a storage container no larger than 2 ft x 3 ft x 5 ft.

5. Safety considerations for systems operations are critical. A complete safety assessment for the system is required.

6. The Technology Demonstrator will be a full sized prototype of the actual design and must be used to validate the most critical range/payload condition for the aircraft.

7. Takeoff must be accomplished within the 75 ft takeoff region shown on Figure 2.

8. The design team must make provisions for estimating fuel burned, flight speed and distance traveled during the tests. This information is to be monitored from ground based observers.

9. A complete record of prototype production cost (materials and man-hours) is also required.

10. The radio control system and the instrumentation package must be removable and a complete system installation should be able to be accomplished in 30 minutes.

11. System control for the flight demonstrator will be a Futaba 6FG radio system with up to 4 S38 servos or a system of comparable weight and size.

12. All FAA and FCC regulations for operation of remotely piloted vehicles and others imposed by the course instructor must be complied with.

Appendix B

City-to-City Economic
Analysis Tables

City-To-City Tables Explanation *

The data presented in these tables is based on the most expensive fuel price of $120/mah. Figures for the remaining two fuel ranges would be calculated in the same manner.

The information for the distances between cities was provided in the Request for Proposal. The longest distance (city A to city N, 9035 feet) was selected and the cost for this flight was calculated (see main text under **ECONOMICS** for this cost explanation). It was decided that breaking even at half capacity (25 passengers) would be the most desirable. The cost for flight was divided by these 25 passengers to determine the cost of a ticket. The ticket price was converted to a price per 50 feet scale to be consistent with given ship and train fares. This price per 50 feet was then applied to all city-to-city travel and resulting prices are given in the tables that follow.

The cost figures in the cost for flight table were calculated by the following formula for each city-to-city trip:

cost for flight = [(fuel cost per 50 feet) + (maintenance cost per 50 feet)] * distance

Next the profit for flights between cities was calculated assuming a full aircraft. The cost for flight was subtracted from the ticket price multiplied by 51 passengers for each city and presented in the tables.

The tables for load factor and number of passengers to break even represent the same information in different terms. To determine these figures the cost for flight between each city was divided by the

ticket price for that flight. This gives a number to break even and this is converted to a percentage of the full capacity of the aircraft to be presented as the load factor.

DISTANCE BETWEEN CITIES

	A	B	C	D	E	F	G	H	I	J	K	L	M	N	O
A	XXXXXXXXXX	1697.05627	3111.26984	5122.49939	6161.16872	3492.84984	3883.29757	4176.1226	5803.44725	5502.7266	6390.61812	8395.23674	8202.43866	9035.4856	8731.55198
B	1697.05627	XXXXXXXXXX	3544.00903	5215.36192	5458.93763	2236.06798	2236.06798	2800	4707.44092	4044.74968	4903.06027	7025.66723	7138.62732	7810.24968	8163.33265
C	3111.26984	3544.00903	XXXXXXXXXX	2059.12603	3883.29757	3231.09888	4512.20567	3847.07681	4326.66153	5000	5813.77674	7211.10255	6324.55532	7432.36167	6053.09838
D	5122.49939	5215.36192	2059.12603	XXXXXXXXXX	2690.72481	4044.74968	5458.93763	4400	3847.07681	5141.98405	5758.47202	6529.93109	5161.39516	6403.12424	4204.75921
E	6161.16872	5458.93763	3883.29757	2690.72481	XXXXXXXXXX	3405.87727	4560.7017	3280.24389	1612.45155	3298.4845	3600	3883.29757	2505.99282	3720.21505	2720.2941
F	3492.84984	2236.06798	3231.09888	4044.74968	3405.87727	XXXXXXXXXX	1414.21356	721.110255	2473.86338	2059.12603	2952.96461	4903.06027	4903.06027	5600	6122.09115
G	3883.29757	2236.06798	4512.20567	5458.93763	4560.7017	1414.21356	XXXXXXXXXX	1280.62485	3280.24389	2039.60781	2800	5015.97448	5546.16985	5966.57356	7213.87552
H	4176.1226	2800	3847.07681	4400	3280.24389	721.110255	1280.62485	XXXXXXXXXX	2059.12603	1341.64079	2236.06798	4242.64069	4427.18872	5015.97448	5939.69696
I	5803.44725	4707.44092	4326.66153	3847.07681	1612.45155	2473.86338	3280.24389	2059.12603	XXXXXXXXXX	1708.80075	2009.97512	2884.44102	2433.10501	3255.76412	4000
J	5502.7266	4044.74968	5000	5141.98405	3298.4845	2059.12603	2039.60781	1341.64079	1708.80075	XXXXXXXXXX	894.427191	3000	3605.55128	3929.37654	5660.38868
K	6390.61812	4903.06027	5813.77674	5758.47202	3600	2952.96461	2800	2236.06798	2009.97512	894.427191	XXXXXXXXXX	2236.06798	3255.76412	3310.58907	5646.23769
L	8395.23674	7025.66723	7211.10255	6529.93109	3883.29757	4903.06027	5015.97448	4242.64069	2884.44102	3000	2236.06798	XXXXXXXXXX	2000	1280.62485	4800
M	8202.43866	7138.62732	6324.55532	5161.39516	2505.99282	4903.06027	5546.16985	4427.18872	2433.10501	3605.55128	3255.76412	2000	XXXXXXXXXX	1280.62485	2800
N	9035.4856	7810.24968	7432.36167	6403.12424	3720.21505	5600	5966.57356	5015.97448	3255.76412	3929.37654	3310.58907	1280.62485	1280.62485	XXXXXXXXXX	3883.29757
O	8731.55198	8163.33265	6053.09838	4204.75921	2720.2941	6122.09115	7213.87552	5939.69696	4000	5660.38868	5646.23769	4800	2800	3883.29757	XXXXXXXXXX

TICKET PRICE

	A	B	C	D	E	F	G	H	I	J	K	L	M	N	O
A	XXXXXXXXXX	$426.75	$740.70	$1,187.19	$1,417.78	$825.41	$912.09	$977.10	$1,338.37	$1,271.61	$1,468.72	$1,913.74	$1,870.94	$2,055.88	$1,988.40
B	$426.75	XXXXXXXXXX	$836.77	$1,207.81	$1,261.88	$546.41	$546.41	$671.60	$1,095.05	$947.93	$1,138.48	$1,609.70	$1,634.78	$1,783.88	$1,862.26
C	$740.70	$836.77	XXXXXXXXXX	$507.13	$912.09	$767.30	$1,051.71	$904.05	$1,010.52	$1,160.00	$1,340.66	$1,650.86	$1,454.05	$1,699.98	$1,393.79
D	$1,187.19	$1,207.81	$507.13	XXXXXXXXXX	$647.34	$947.93	$1,261.88	$1,026.80	$904.05	$1,191.52	$1,328.38	$1,499.64	$1,195.83	$1,471.49	$983.46
E	$1,417.78	$1,261.88	$912.09	$647.34	XXXXXXXXXX	$806.10	$1,062.48	$778.21	$407.96	$782.26	$849.20	$912.09	$606.33	$875.89	$653.91
F	$825.41	$546.41	$767.30	$947.93	$806.10	XXXXXXXXXX	$363.96	$210.09	$599.20	$507.13	$705.56	$1,138.48	$1,138.48	$1,293.20	$1,409.10
G	$912.09	$546.41	$1,051.71	$1,261.88	$1,062.48	$363.96	XXXXXXXXXX	$334.30	$778.21	$502.79	$671.60	$1,163.55	$1,281.25	$1,374.58	$1,651.48
H	$977.10	$671.60	$904.05	$1,026.80	$778.21	$210.09	$334.30	XXXXXXXXXX	$507.13	$347.84	$546.41	$991.87	$1,032.84	$1,163.55	$1,368.61
I	$1,338.37	$1,095.05	$1,010.52	$904.05	$407.96	$599.20	$778.21	$507.13	XXXXXXXXXX	$429.35	$496.21	$690.35	$590.15	$772.78	$938.00
J	$1,271.61	$947.93	$1,160.00	$1,191.52	$782.26	$507.13	$502.79	$347.84	$429.35	XXXXXXXXXX	$248.56	$716.00	$850.43	$922.32	$1,306.61
K	$1,468.72	$1,138.48	$1,340.66	$1,328.38	$849.20	$705.56	$671.60	$546.41	$496.21	$248.56	XXXXXXXXXX	$546.41	$772.78	$784.95	$1,303.46
L	$1,913.74	$1,609.70	$1,650.86	$1,499.64	$912.09	$1,138.48	$1,163.55	$991.87	$690.35	$716.00	$546.41	XXXXXXXXXX	$494.00	$334.30	$1,115.60
M	$1,870.94	$1,634.78	$1,454.05	$1,195.83	$606.33	$1,138.48	$1,281.25	$1,032.84	$590.15	$850.43	$772.78	$494.00	XXXXXXXXXX	$334.30	$671.60
N	$2,055.88	$1,783.88	$1,699.98	$1,471.49	$875.89	$1,293.20	$1,374.58	$1,163.55	$772.78	$922.32	$784.95	$334.30	$334.30	XXXXXXXXXX	$912.09
O	$1,988.40	$1,862.26	$1,393.79	$983.46	$653.91	$1,409.10	$1,651.48	$1,368.61	$938.00	$1,306.61	$1,303.46	$1,115.60	$671.60	$912.09	XXXXXXXXXX

COST FOR FLIGHT ($120/mah)

	A	B	C	D	E	F	G	H	I	J	K	L	M	N	O
A	XXXXXXXXXX	$9,842.93	$18,045.37	$29,710.50	$35,734.78	$20,258.53	$22,523.13	$24,221.51	$33,659.99	$31,915.81	$37,065.59	$48,692.37	$47,574.14	$52,405.82	$50,643.00
B	$9,842.93	XXXXXXXXXX	$20,555.25	$30,249.10	$31,661.84	$12,969.19	$12,969.19	$16,240.00	$27,303.16	$23,459.55	$28,437.75	$40,748.87	$41,404.04	$45,299.45	$47,347.33
C	$18,045.37	$20,555.25	XXXXXXXXXX	$11,942.93	$22,523.13	$18,740.37	$26,170.79	$22,313.05	$25,094.64	$29,000.00	$33,719.91	$41,824.39	$36,682.42	$43,107.70	$35,107.97
D	$29,710.50	$30,249.10	$11,942.93	XXXXXXXXXX	$15,606.20	$23,459.55	$31,661.84	$25,520.00	$22,313.05	$29,823.51	$33,399.14	$37,873.60	$29,936.09	$37,138.12	$24,387.60
E	$35,734.78	$31,661.84	$22,523.13	$15,606.20	XXXXXXXXXX	$19,754.09	$26,452.07	$19,025.41	$9,352.22	$19,131.21	$20,880.00	$22,523.13	$14,534.76	$21,577.25	$15,777.71
F	$20,258.53	$12,969.19	$18,740.37	$23,459.55	$19,754.09	XXXXXXXXXX	$8,202.44	$4,182.44	$14,348.41	$11,942.93	$17,127.19	$28,437.75	$28,437.75	$32,480.00	$35,508.13
G	$22,523.13	$12,969.19	$26,170.79	$31,661.84	$26,452.07	$8,202.44	XXXXXXXXXX	$7,427.62	$19,025.41	$11,829.73	$16,240.00	$29,092.65	$32,167.79	$34,606.13	$41,840.48
H	$24,221.51	$16,240.00	$22,313.05	$25,520.00	$19,025.41	$4,182.44	$7,427.62	XXXXXXXXXX	$11,942.93	$7,781.52	$12,969.19	$24,607.32	$25,677.69	$29,092.65	$34,450.24
I	$33,659.99	$27,303.16	$25,094.64	$22,313.05	$9,352.22	$14,348.41	$19,025.41	$11,942.93	XXXXXXXXXX	$9,911.04	$16,729.76	$14,112.01	$18,883.43	$23,200.00	
J	$31,915.81	$23,459.55	$29,000.00	$29,823.51	$19,131.21	$11,942.93	$11,829.73	$7,781.52	$9,911.04	XXXXXXXXXX	$5,187.68	$17,400.00	$20,912.20	$22,790.38	$32,830.25
K	$37,065.59	$28,437.75	$33,719.91	$33,399.14	$20,880.00	$17,127.19	$16,240.00	$12,969.19	$11,657.86	$5,187.68	XXXXXXXXXX	$12,969.19	$18,883.43	$19,201.42	$32,748.18
L	$48,692.37	$40,748.87	$41,824.39	$37,873.60	$22,523.13	$28,437.75	$29,092.65	$24,607.32	$16,729.76	$17,400.00	$12,969.19	XXXXXXXXXX	$11,600.00	$7,427.62	$27,840.00
M	$47,574.14	$41,404.04	$36,682.42	$29,936.09	$14,534.76	$28,437.75	$32,167.79	$25,677.69	$14,112.01	$20,912.20	$18,883.43	$11,600.00	XXXXXXXXXX	$7,427.62	$16,240.00
N	$52,405.82	$45,299.45	$43,107.70	$37,138.12	$21,577.25	$32,480.00	$34,606.13	$29,092.65	$18,883.43	$22,790.38	$19,201.42	$7,427.62	$7,427.62	XXXXXXXXXX	$22,523.13
O	$50,643.00	$47,347.33	$35,107.97	$24,387.60	$15,777.71	$35,508.13	$41,840.48	$34,450.24	$23,200.00	$32,830.25	$32,748.18	$27,840.00	$16,240.00	$22,523.13	XXXXXXXXXX

NUMBER OF PASSENGERS TO BREAK EVEN ($120/mah)

	A	B	C	D	E	F	G	H	I	J	K	L	M	N	O
A	XXXXXXXXXXX	23.1	24.4	25	25.2	24.5	24.7	24.8	25.2	25.1	25.2	25.4	25.4	25.5	25.5
B	23.1	XXXXXXXXXXX	24.6	25	25.1	23.7	23.7	24.2	24.9	24.7	25	25.3	25.3	25.4	25.4
C	24.4	24.6	XXXXXXXXXXX	23.6	24.7	24.4	24.9	24.7	24.8	25	25.2	25.3	25.2	25.4	25.2
D	25	25	23.6	XXXXXXXXXXX	24.1	24.7	25.1	24.9	24.7	25	25.1	25.3	25	25.2	24.8
E	25.2	25.1	24.7	24.1	XXXXXXXXXXX	24.5	24.9	24.4	22.9	24.5	24.6	24.7	24	24.6	24.1
F	24.5	23.7	24.4	24.7	24.5	XXXXXXXXXXX	22.5	19.9	23.9	23.6	24.3	25	25	25.1	25.2
G	24.7	23.7	24.9	25.1	24.9	22.5	XXXXXXXXXXX	22.2	24.4	23.5	24.2	25	25.1	25.2	25.3
H	24.8	24.2	24.7	24.9	24.4	19.9	22.2	XXXXXXXXXXX	23.6	22.4	23.7	24.8	24.9	25	25.2
I	25.2	24.9	24.8	24.7	22.9	23.9	24.4	23.6	XXXXXXXXXXX	23.1	23.5	24.2	23.9	24.4	24.7
J	25.1	24.7	25	25	24.5	23.6	23.5	22.4	23.1	XXXXXXXXXXX	20.9	24.3	24.6	24.7	25.1
K	25.2	25	25.2	25.1	24.6	24.3	24.2	23.7	23.5	20.9	XXXXXXXXXXX	23.7	24.4	24.5	25.1
L	25.4	25.3	25.3	25.3	24.7	25	25	24.8	24.2	24.3	23.7	XXXXXXXXXXX	23.5	22.2	25
M	25.4	25.3	25.2	25	24	25	25.1	24.9	23.9	24.6	24.4	23.5	XXXXXXXXXXX	22.2	24.2
N	25.5	25.4	25.4	25.2	24.6	25.1	25.2	25	24.4	24.7	24.5	22.2	22.2	XXXXXXXXXXX	24.7
O	25.5	25.4	25.2	24.8	24.1	25.2	25.3	25.2	24.7	25.1	25.1	25	24.2	24.7	XXXXXXXXXXX

TOTAL PROFIT - 51 pass. ($120/mah)

	A	B	C	D	E	F	G	H	I	J	K	L	M	N	O
A	XXXXXXXXXXX	$11,921.14	$19,730.43	$30,836.44	$36,571.97	$21,837.52	$23,993.57	$25,610.55	$34,596.64	$32,936.06	$37,838.99	$48,908.50	$47,843.87	$52,443.95	$50,765.63
B	$11,921.14	XXXXXXXXXXX	$22,120.02	$31,349.23	$32,694.25	$14,897.57	$14,897.57	$18,011.60	$28,544.49	$24,885.11	$29,624.70	$41,345.73	$41,969.50	$45,678.20	$47,627.92
C	$19,730.43	$22,120.02	XXXXXXXXXXX	$13,920.49	$23,993.57	$20,392.13	$27,466.40	$23,793.56	$26,441.82	$30,160.00	$34,653.68	$42,369.71	$37,474.19	$43,591.50	$35,975.21
D	$30,836.44	$31,349.23	$13,920.49	XXXXXXXXXXX	$17,408.18	$24,885.11	$32,694.25	$26,846.80	$23,793.56	$30,944.04	$34,348.28	$38,608.28	$31,051.22	$37,908.05	$25,768.68
E	$36,571.97	$32,694.25	$23,993.57	$17,408.18	XXXXXXXXXXX	$21,357.25	$27,734.19	$20,663.51	$11,453.96	$20,764.23	$22,429.20	$23,993.57	$16,388.09	$23,093.03	$17,571.46
F	$21,837.52	$14,897.57	$20,392.13	$24,885.11	$21,357.25	XXXXXXXXXXX	$10,359.29	$6,531.97	$16,210.67	$13,920.49	$18,856.27	$29,624.70	$29,624.70	$33,473.20	$36,356.19
G	$23,993.57	$14,897.57	$27,466.40	$32,694.25	$27,734.19	$10,359.29	XXXXXXXXXXX	$9,621.61	$20,663.51	$13,812.71	$18,011.60	$30,248.21	$33,175.95	$35,497.42	$42,385.02
H	$25,610.55	$18,011.60	$23,793.56	$26,846.80	$20,663.51	$6,531.97	$9,621.61	XXXXXXXXXXX	$13,920.49	$9,958.54	$14,897.57	$25,977.86	$26,996.94	$30,248.21	$35,349.01
I	$34,596.64	$28,544.49	$26,441.82	$23,793.56	$11,453.96	$16,210.67	$20,663.51	$13,920.49	XXXXXXXXXXX	$11,986.00	$13,649.08	$18,477.88	$15,985.61	$20,528.33	$24,638.00
J	$32,936.06	$24,885.11	$30,160.00	$30,944.04	$20,764.23	$13,920.49	$13,812.71	$9,958.54	$11,986.00	XXXXXXXXXXX	$7,489.03	$19,116.00	$22,459.85	$24,248.02	$33,806.67
K	$37,838.99	$29,624.70	$34,653.68	$34,348.28	$22,429.20	$18,856.27	$18,011.60	$14,897.57	$13,649.08	$7,489.03	XXXXXXXXXXX	$14,897.57	$20,528.33	$20,831.07	$33,728.52
L	$48,908.50	$41,345.73	$42,369.71	$38,608.28	$23,993.57	$29,624.70	$30,248.21	$25,977.86	$18,477.88	$19,116.00	$14,897.57	XXXXXXXXXXX	$13,594.00	$9,621.61	$29,055.60
M	$47,843.87	$41,969.50	$37,474.19	$31,051.22	$16,388.09	$29,624.70	$33,175.95	$26,996.94	$15,985.61	$22,459.85	$20,528.33	$13,594.00	XXXXXXXXXXX	$9,621.61	$18,011.60
N	$52,443.95	$45,678.20	$43,591.50	$37,908.05	$23,093.03	$33,473.20	$35,497.42	$30,248.21	$20,528.33	$24,248.02	$20,831.07	$9,621.61	$9,621.61	XXXXXXXXXXX	$23,993.57
O	$50,765.63	$47,627.92	$35,975.21	$25,768.68	$17,571.46	$36,356.19	$42,385.02	$35,349.01	$24,638.00	$33,806.67	$33,728.52	$29,055.60	$18,011.60	$23,993.57	XXXXXXXXXXX

PASSENGER LOAD FACTOR ($120/MAH)

	A	B	C	D	E	F	G	H	I	J	K	L	M	N	O
A	XXXXXXXXXXX	45.23%	47.77%	49.07%	49.42%	48.12%	48.42%	48.61%	49.31%	49.21%	49.48%	49.89%	49.86%	49.98%	49.94%
B	45.23%	XXXXXXXXXXX	48.17%	49.11%	49.20%	46.54%	46.54%	47.41%	48.89%	48.53%	48.98%	49.64%	49.66%	49.79%	49.85%
C	47.77%	48.17%	XXXXXXXXXXX	46.18%	48.42%	47.89%	48.79%	48.39%	48.69%	49.02%	49.32%	49.68%	49.47%	49.72%	49.39%
D	49.07%	49.11%	46.18%	XXXXXXXXXXX	47.27%	48.53%	49.20%	48.73%	48.39%	49.08%	49.30%	49.52%	49.09%	49.49%	48.62%
E	49.42%	49.20%	48.42%	47.27%	XXXXXXXXXXX	48.05%	48.82%	47.94%	44.95%	47.95%	48.21%	48.42%	47.00%	48.30%	47.31%
F	48.12%	46.54%	47.89%	48.53%	48.05%	XXXXXXXXXXX	44.19%	39.04%	46.95%	46.18%	47.60%	48.98%	48.98%	49.25%	49.41%
G	48.42%	46.54%	48.79%	49.20%	48.82%	44.19%	XXXXXXXXXXX	43.57%	47.94%	46.13%	47.41%	49.03%	49.23%	49.36%	49.68%
H	48.61%	47.41%	48.39%	48.73%	47.94%	39.04%	43.57%	XXXXXXXXXXX	46.18%	43.86%	46.54%	48.65%	48.75%	49.03%	49.36%
I	49.31%	48.89%	48.69%	48.39%	44.95%	46.95%	47.94%	46.18%	XXXXXXXXXXX	45.26%	46.07%	47.52%	46.89%	47.91%	48.50%
J	49.21%	48.53%	49.02%	49.08%	47.95%	46.18%	46.13%	43.86%	45.26%	XXXXXXXXXXX	40.92%	47.65%	48.22%	48.45%	49.27%
K	49.48%	48.98%	49.32%	49.30%	48.21%	47.60%	47.41%	46.54%	46.07%	40.92%	XXXXXXXXXXX	46.54%	47.91%	47.96%	49.26%
L	49.89%	49.64%	49.68%	49.52%	48.42%	48.98%	49.03%	48.65%	47.52%	47.65%	46.54%	XXXXXXXXXXX	46.04%	43.57%	48.93%
M	49.86%	49.66%	49.47%	49.09%	47.00%	48.98%	49.23%	48.75%	46.89%	48.22%	47.91%	46.04%	XXXXXXXXXXX	43.57%	47.41%
N	49.98%	49.79%	49.72%	49.49%	48.30%	49.25%	49.36%	49.03%	47.91%	48.45%	47.96%	43.57%	43.57%	XXXXXXXXXXX	48.42%
O	49.94%	49.85%	49.39%	48.62%	47.31%	49.41%	49.68%	49.36%	48.50%	49.27%	49.26%	48.93%	47.41%	48.42%	XXXXXXXXXXX

D. References

1. Anderson, John D. Jr. *Introduction to Flight.* New York: Mc Graw-Hill Book Company, 1985.

2. Jensen, Daniel T. "A Drag Prediction Methodology For Low Reynolds Number Flight Vehicles." Thesis submitted to the Graduate School of the University of Notre Dame, Department of Aerospace and Mechanical Engineering. Notre Dame, IN, January, 1990.

3. Nelson, R. C. "Atmospheric Flight Mechanics" University of Notre Dame,
Department of Aerospace and Mechanical Engineering. Notre Dame, IN.

4. Roskam, Dr. Jan. Airplane Design Part VI: *Preliminary Calculation of Aerodynamic, Thrust and Power Characteristics.* Ottawa, Kansas: Roskam Aviation and Engineering Corporation, 1987.

5. Selig, Michael S., Donovan, John F., and Fraser, David B. *Airfoils at Low Speeds.* Virginia Beach, Virginia: H. A. Stokely, Publisher, 1989.

E. References

1. J.D. Anderson, Introduction to Flight, pp. 264-269, McGraw Hill Book Company, New York, NY (1985).

2. F.J. Hale, Introduction to Aircraft Performance, Selection, and Design, pp. 67,68, John Wiley & Sons, New York, NY (1984).

3. R.C. Nelson, "Design Lab Notebook", pp. all, Dept. of Aero & Mech Engineering (UND), Notre Dame, IN (1991).

4. P.F. Dunn, "AE 454 - Lecture 18", pp. all, Dept. of Aero & Mech. Engineering (UND), Notre Dame, IN (1990).

G. References

1. Nelson, R. C. Flight Stability andf Automatic Control. McGraw-Hill, Inc., St. Louis, 1989.

2. Baron-Rawdon, B. "Dihedral." Model Aviation. Aug-Sept-Oct-Nov, 1989.

3. F.J. Hale, Introduction to Aircraft Performance, Selection, and Design, pp. 67,68, John Wiley & Sons, New York, NY (1984).

K. References

1. Hoerner, Sighard F. Fluid-Dynamic Drag. Midland Park, New Jersey, 1958.

2. Roskam, Dr. Jan. Airplane Design. Part III: "Layout Design of Cockpit, Fuselage, Wing and Empennage: Cutaways and Inboard Profiles." University of Kansas, 1987.

3. Roskam, Dr. Jan. Airplane Design. Part IV: "Preliminary Calculation of Aerodynamic, Thrust and Power Characteristics." University of Kansas, 1987.